V. Dolejsi

On the Discontinuous Galerkin Method for the Numerical Solution of the Euler and the Navier–Stokes Equations

Preprint No. MATH-knm-2002/2

08.11.2002

Submitted to *Int. J. Numer. Methods Fluids*

Department of Numerical Mathematics, Faculty of Mathematics and Physics, Charles University, Sokolovská 83, 186 75 Praha 8, Czech Republic

http://www.karlin.mff.cuni.cz/ms-preprints/

Cover print by Reprostředisko, Malostranské nám. 25, Praha 1 - Malá Strana
Design by Mirko Rokyta, picture of snowflake by Ondřej Kalenda
Current series administrator: V. Dolejsi

On the Discontinuous Galerkin Method for the Numerical Solution of the Euler and the Navier–Stokes Equations [1]

V. Dolejší

Abstract

The paper deals with the use of the discontinuous Galerkin finite element method (DG FE) for the numerical solution of compressible flows. We start with a scalar convection-diffusion equation and present a discretization with the aid of the antisymmetric variant of DG FE. We also mention some theoretical results. Then we extend the scheme to the system of the Euler and Navier-Stokes equations. The use of order limiting in vicinity of discontinuities and steep gradients and the use of superparametric finite elements are discussed. Several numerical examples are presented.

Keywords: discontinuous Galerkin finite element method, methods of lines, convection-diffusion problems, limiting of order of accuracy, compressible flow

MSC Classification 2000: 65M60, 65M20, 76M10

1 Introduction

Our goal is to develop a suitable method for the numerical solution of compressible flows. During last years we have dealt with combined finite volume (FV) – finite element (FE) methods which give good results in many cases of technically relevant problems in complex domains. For analysis and applications, see, e. g., [1], [18], [19], [22], [20], [21]. However, their drawback is the necessity to construct two mutually associated meshes, which is rather complicated particularly in 3D ([23]). Moreover, these schemes, which are only of the first order of accuracy, suffer from a high amount of numerical viscosity. For problems with a small physical viscosity, the numerical viscosity dominates and we can not obtain satisfactory results. In order to avoid such difficulties, the use of a higher order scheme is necessary.

A generalization of FV and FE methods is the discontinuous Galerkin finite element (DG FE) method based on piecewise polynomial approximations without any requirement on the interelement continuity. It uses only one mesh and allows higher order of accuracy. Recently, the DG FE method has become quite popular and is discussed in a number of papers. For a survey about DG FE methods, see, [8] or [9]. Let us mention particularly the papers [6] and [25] on theoretical analysis of this method applied to linear problems. The works [3] and [4] deal with the numerical simulation of compressible flows with the aid of DG FE method, where the viscous terms are treated with the mixed formulation. Another approcah of the numerical solution of the Euler and Navier–Stokes equations is given in the paper [5], which is concerned with a discontinuous hp finite element method.

[1] This work was supported under the grants No. 201/02/0684 and No. 201/00/D116 of the Czech Grant Agency and by the Grant MSM 113200007. The author acknowledges this support.

Various numerical experiments indicate that the DG FE method is particularly suitable for the numerical solution of nonlinear conservation laws with discontinuous solutions and nonlinear convection-diffusion problems whose solutions have steep gradients. This is the subject of this paper. Our goal is to develop sufficiently accurate and robust numerical schemes for nonlinear conservation laws and convection-diffusion problems which produce numerical solutions not suffering from the so-called spurious oscillations in the vicinity of discontinuities and steep gradients. The main applications are oriented to the simulation of compressible high-speed flow.

In [13] and [12] we developed two methods for scalar nonlinear convection-diffusion problems. Here our main emphasis is put on the extension to the Euler and the Navier-Stokes equations, which describe inviscid and viscous gas flow, respectively. The presented scheme is similar to the scheme from [5], the difference is that we include into the scheme the stabilization term J_h^σ given by (2.17). This stabilization term and the order limitation allow us to resolve problems containing discontinuities or steep gradients, e.g., transonic flows.

The contents of the paper is the following. In Section 2 we deal with the numerical solution of a scalar convection-diffusion equation with the aid of the DG FE method. We present a numerical scheme and mention some theoretical results concerning a priori error estimates. In Section 3 we extend the numerical scheme to the systems of the Euler and Navier-Stokes equations. In order to obtain a physically relevant numerical solution, we use an order limiting in vicinity of singularities (Section 4) and the superparametric finite elements (Section 5). Several numerical examples are given in Section 6.

2 Scalar convection-diffusion equation

We start with the numerical solution of a scalar equation. Following [13] and [12] we briefly derive a numerical scheme based on the DG FE discretization.

2.1 Continuous problem

Let $\Omega \subset \mathbb{R}^d$ ($d = 2$ or 3) be a bounded polyhedral domain and $T > 0$. We set $Q_T = \Omega \times (0,T)$ and by $\partial\Omega$ we denote the boundary of Ω which consists of two disjoint parts $\partial\Omega_D$ and $\partial\Omega_N$. We consider the following *initial-boundary value problem*: Find $u : Q_T \to \mathbb{R}$ such that

$$\frac{\partial u}{\partial t} + \sum_{s=1}^{d} \frac{\partial f_s(u)}{\partial x_s} = \sum_{s=1}^{d} \frac{\partial R_s(u, \nabla u)}{\partial x_s} + g \quad \text{in } Q_T, \tag{2.1}$$

$$u(x,t) = u_D(x) \quad \text{for } x \in \partial\Omega_D, t \in (0,T), \tag{2.2}$$

$$\sum_{s=1}^{d} R_s(u, \nabla u) n_s = g_N \quad \text{for } x \in \partial\Omega_N, t \in (0,T), \tag{2.3}$$

$$u(x,0) = u^0(x), \quad x \in \Omega. \tag{2.4}$$

Here $x = (x_1, \dots, x_d)$ and t denotes the space and time coordinates and $\boldsymbol{n} = (n_1, \dots, n_d)$ is a unit outer normal to $\partial\Omega$. We suppose that $f_s \in C^1(\mathbb{R})$, $R_s \in$

$C^1(\mathbb{R}^{d+1}), R_s(u,\alpha)$ is linear with respect to $\alpha \in \mathbb{R}^d$ and the data are sufficiently regular so that we can assume the existence of a *strong solution* u satisfying (2.1) – (2.4) pointwise almost everywhere.

We use the standard notation for function spaces: $H^k(\Omega)$ = Sobolev space, $L^2(0,T;X)$ = Bochner space of square integrable functions on $(0,T)$ with values in a Banach space X, $C^1(0,T;X)$ = space of continuously differentiable mappings in $(0,T)$ with values in X.

2.2 Discretization

Let $\mathcal{T}_h$ $(h > 0)$ denotes a partition of the closure $\overline{\Omega}$ of the domain Ω into a finite number of closed d-dimensional convex polyhedra K with mutually disjoint interiors. We call $\mathcal{T}_h$ a triangulation of $\overline{\Omega}$, but *do not* require the usual conforming properties from the finite element method. In 2D problems we choose usually $K \in \mathcal{T}_h$ as triangles or quadrilaterals. In 3D, $K \in \mathcal{T}_h$ can be, e. g., tetrahedra, pyramids or hexahedra. We can allow even more general elements K.

We set $h_K = \mathrm{diam}(K)$, $h = \max_{K\in\mathcal{T}_h} h_K$. By $|K|$ we denote the d-dimensional Lebesgue measure of K. All elements of $\mathcal{T}_h$ will be numbered so that $\mathcal{T}_h = \{K_i\}_{i\in I}$, where $I \subset Z^+ = \{1,2,\ldots\}$ is a suitable index set. If two elements K_i, $K_j \in \mathcal{T}_h$ contain a nonempty open face which is a part of a $(d-1)$-dimensional hyperplane, we call them *neighbours*. We set in this case $\Gamma_{ij} = \partial K_i \cap \partial K_j$ and assume that the whole set Γ_{ij} is a part of a $(d-1)$-dimensional hyperplane. For $i \in I$ we set $s(i) = \{j \in I; K_j \text{ is a neighbour of } K_i\}$.

The boundary $\partial\Omega$ is formed by a finite number of faces of elements K_i adjacent to $\partial\Omega$. We denote all these boundary faces by S_j, where $j \in I_b \subset Z^- = \{-1,-2,\ldots\}$ and set $\gamma(i) = \{j \in I_b; S_j \text{ is a face of } K_i\}, \Gamma_{ij} = S_j$ for $K_i \in \mathcal{T}_h$ such that $S_j \subset \partial K_i$, $j \in I_b$. For K_i not containing any boundary face S_j we set $\gamma(i) = \emptyset$. Obviously, $s(i) \cap \gamma(i) = \emptyset$ for all $i \in I$. Now, if we write $S(i) = s(i) \cup \gamma(i)$, we have

$$\partial K_i = \bigcup_{j\in S(i)} \Gamma_{ij}, \qquad \partial K_i \cap \partial\Omega = \bigcup_{j\in\gamma(i)} \Gamma_{ij}. \tag{2.5}$$

Moreover, we define two subsets $\gamma_D(i)$ and $\gamma_N(i)$ corresponding to $\partial\Omega_D$ and $\partial\Omega_N$ parts of boundary, respectively. Obviously,

$$\gamma(i) = \gamma_D(i) \cup \gamma_N(i) \quad \text{and} \quad \gamma_D(i) \cap \gamma_N(i) = \emptyset. \tag{2.6}$$

Furthermore, we use the following notation: $\boldsymbol{n}_{ij} = ((n_{ij})_1, ..., (n_{ij})_d)$ = unit outer normal to ∂K_i on the face Γ_{ij}, $d(\Gamma_{ij}) = \mathrm{diam}(\Gamma_{ij}), |\Gamma_{ij}| = (d-1)-$ dimensional Lebesgue measure of Γ_{ij}.

Over the triangulation $\mathcal{T}_h$ we define the *broken Sobolev space*

$$H^k(\Omega,\mathcal{T}_h) = \{v; v|_K \in H^k(K)\ \forall\, K \in \mathcal{T}_h\}. \tag{2.7}$$

For $v \in H^1(\Omega,\mathcal{T}_h)$ we introduce the following notation

$$\begin{aligned} v|_{\Gamma_{ij}} &= \text{the trace of } v|_{K_i} \text{on } \Gamma_{ij}, \\ v|_{\Gamma_{ji}} &= \text{the trace of } v|_{K_j} \text{on } \Gamma_{ji} = \Gamma_{ij}, \end{aligned} \tag{2.8}$$

$$\begin{aligned}\langle v\rangle_{\Gamma_{ij}} &= \frac{1}{2}\left(v|_{\Gamma_{ij}} + v|_{\Gamma_{ji}}\right),\\ [v]_{\Gamma_{ij}} &= v|_{\Gamma_{ij}} - v|_{\Gamma_{ji}}.\end{aligned}$$

Obviously, $\langle v\rangle_{\Gamma_{ij}} = \langle v\rangle_{\Gamma_{ji}}$, but $[v]_{\Gamma_{ij}} = -[v]_{\Gamma_{ji}}$ and $[v]_{\Gamma_{ij}}\boldsymbol{n}_{ij} = [v]_{\Gamma_{ji}}\boldsymbol{n}_{ji}$.

The approximate solution of problem (2.1) – (2.4) is sought in the space of discontinuous piecewise polynomial functions

$$S_h = S^{p,-1}(\Omega, \mathcal{T}_h) = \{v; v|_K \in P_p(K)\ \forall\, K \in \mathcal{T}_h\}, \tag{2.9}$$

where $P_p(K)$ denotes the space of all polynomials on K of degree $\le p$.

In order to derive the discrete problem, we start from a strong solution u such that $u \in L^2((0,T), H^2(\Omega))$ and $\frac{\partial u}{\partial t} \in L^2((0,T), H^2(\Omega))$. We multiply equation (2.1) by any $\varphi \in H^2(\Omega, \mathcal{T}_h)$, integrate over $K \in \mathcal{T}_h$, apply Green's theorem and sum over all $K \in \mathcal{T}_h$. Moreover, we use the relations $\langle \nabla u\rangle_{\Gamma_{ij}} = \nabla u|_{\Gamma_{ij}} = \nabla u|_{\Gamma_{ji}}$ and the identities

$$\int_{\Gamma_{ij}} \sum_{s=1}^{d} \langle R_s(u, \nabla\varphi)\rangle\, (n_{ij})_s\, [u]\, \mathrm{d}S = 0,\ \int_{\Gamma_{ij}} [u][\varphi]\, \mathrm{d}S = 0 \quad \forall j \in s(i) \forall i \in I. \tag{2.10}$$

Furthermore, adding some terms which mutually cancel, we find that

$$\begin{aligned}
&\int_\Omega \frac{\partial u}{\partial t}\,\varphi\,\mathrm{d}x + \sum_{i\in I}\sum_{j\in S(i)} \int_{\Gamma_{ij}} \sum_{s=1}^{d} f_s(u)\,(n_{ij})_s\,\varphi|_{\Gamma_{ij}}\,\mathrm{d}S\\
&- \sum_{i\in I}\int_{K_i}\sum_{s=1}^{d} f_s(u)\,\frac{\partial\varphi}{\partial x_s}\,\mathrm{d}x + \sum_{i\in I}\int_{K_i}\sum_{s=1}^{d} R_s(u,\nabla u))\,\frac{\partial\varphi}{\partial x_s}\,\mathrm{d}x\\
&- \sum_{i\in I}\sum_{\substack{j\in s(i)\\ j<i}}\int_{\Gamma_{ij}}\sum_{s=1}^{d}\langle R_s(u,\nabla u)\rangle\,(n_{ij})_s\,[\varphi]\,\mathrm{d}S\\
&+ \sum_{i\in I}\sum_{\substack{j\in s(i)\\ j<i}}\int_{\Gamma_{ij}}\sum_{s=1}^{d}\langle R_s(u,\nabla\varphi)\rangle\,(n_{ij})_s\,[u]\,\mathrm{d}S\\
&- \sum_{i\in I}\sum_{j\in\gamma_D(i)}\int_{\Gamma_{ij}}\sum_{s=1}^{d} R_s(u,\nabla u)\,(n_{ij})_s\,\varphi\,\mathrm{d}S\\
&+ \sum_{i\in I}\sum_{j\in\gamma_D(i)}\int_{\Gamma_{ij}}\sum_{s=1}^{d} R_s(u,\nabla\varphi)\,(n_{ij})_s\,(u-u_D)\,\mathrm{d}S\\
&+ \sum_{i\in I}\sum_{j\in s(i)}\int_{\Gamma_{ij}}\sigma[u]\,[\varphi]\,\mathrm{d}S + \sum_{i\in I}\sum_{j\in\gamma_D(i)}\int_{\Gamma_{ij}}\sigma\,(u-u_D)\,\varphi\,\mathrm{d}S\\
=\ &\int_\Omega g\,\varphi\,\mathrm{d}x + \sum_{i\in I}\sum_{j\in\gamma_N(i)}\int_{\Gamma_{ij}} g_N\,\varphi\,\mathrm{d}S.
\end{aligned} \tag{2.11}$$

Here σ is a weight function defined on each Γ_{ij} by $\sigma|_{\Gamma_{ij}} = \varepsilon/\mathrm{d}(\Gamma_{ij})$, where $\varepsilon \approx R_s$. Let us note that the form (2.11) is an antisymmetric variant of the DG FE

approximation of the diffusion terms proposed in [26], [2] as the terms

$$\sum_{i\in I}\sum_{\substack{j\in s(i)\\ j<i}}\int_{\Gamma_{ij}}\sum_{s=1}^{d}\langle R_s(u,\nabla u)\rangle\,(n_{ij})_s\,[\varphi]\,\mathrm{d}S, \tag{2.12}$$

$$\sum_{i\in I}\sum_{\substack{j\in s(i)\\ j<i}}\int_{\Gamma_{ij}}\sum_{s=1}^{d}\langle R_s(u,\nabla \varphi)\rangle\,(n_{ij})_s\,[u]\,\mathrm{d}S$$

and

$$\sum_{i\in I}\sum_{j\in\gamma_D(i)}\int_{\Gamma_{ij}}\sum_{s=1}^{d}R_s(u,\nabla u)\,(n_{ij})_s\,\varphi\,\mathrm{d}S, \tag{2.13}$$

$$\sum_{i\in I}\sum_{j\in\gamma_D(i)}\int_{\Gamma_{ij}}\sum_{s=1}^{d}R_s(u,\nabla \varphi)\,(n_{ij})_s\,u\,\mathrm{d}S$$

have opposite signs.

Similarly as in the FV method the inviscid fluxes will be approximated with the aid of the so-called numerical flux $H(u,u',\boldsymbol{n})$:

$$\int_{\Gamma_{ij}}\sum_{s=1}^{d}f_s(u_h)\,n_s\,\varphi_h\,\mathrm{d}S\approx\int_{\Gamma_{ij}}H(u_h|_{\Gamma_{ij}},u_h|_{\Gamma_{ji}},\boldsymbol{n}_{ij})\,\varphi_h\,\mathrm{d}S,\ i\in I,\ j\in S(i). \tag{2.14}$$

Of course, if $j\in\gamma(i)$ and $\Gamma_{ij}\subset\partial\Omega$, it is necessary to specify the meaning of $u|_{\Gamma_{ji}}$. Here we use the extrapolation, i.e. we set $u|_{\Gamma_{ji}}:=u|_{\Gamma_{ij}}$. In this way we obtain the convection form $b_h(u,v)$:

$$\begin{aligned} b_h(u_h,\varphi_h) &= \sum_{i\in I}\left(\sum_{j\in s(i)}\int_{\Gamma_{ij}}H(u_h|_{\Gamma_{ij}},u_h|_{\Gamma_{ji}},\boldsymbol{n}_{ij})\,\varphi_h|_{\Gamma_{ij}}\,\mathrm{d}S\right.\\ &\quad\left.+\sum_{j\in\gamma(i)}\int_{\Gamma_{ij}}H(u_h|_{\Gamma_{ij}},u_h|_{\Gamma_{ij}},\boldsymbol{n}_{ij})\,\varphi_h|_{\Gamma_{ij}}\,\mathrm{d}S\right)\\ &\quad-\sum_{i\in I}\int_{K_i}\sum_{s=1}^{d}f_s(u_h)\,\frac{\partial\varphi_h}{\partial x_s}\,\mathrm{d}x,\quad u_h,\,\varphi_h\in H^2(\Omega,\mathcal{T}_h). \end{aligned} \tag{2.15}$$

Now, for $u_h,\varphi_h\in H^2(\Omega,\mathcal{T}_h)$ we set

$$\begin{aligned} a_h(u_h,\varphi_h) &= \sum_{i\in I}\int_{K_i}\sum_{s=1}^{d}R_s(u_h,\nabla u_h))\,\frac{\partial\varphi_h}{\partial x_s}\,\mathrm{d}x\\ &\quad-\sum_{i\in I}\sum_{\substack{j\in S(i)\\ j<i}}\int_{\Gamma_{ij}}\sum_{s=1}^{d}\langle R_s(u_h,\nabla u_h)\rangle\,(n_{ij})_s\,[\varphi_h]\,\mathrm{d}S\\ &\quad+\sum_{i\in I}\sum_{\substack{j\in S(i)\\ j<i}}\int_{\Gamma_{ij}}\sum_{s=1}^{d}\langle R_s(u_h,\nabla \varphi_h)\rangle\,(n_{ij})_s\,[u_h]\,\mathrm{d}S \end{aligned} \tag{2.16}$$

$$
\begin{aligned}
&- \sum_{i\in I} \sum_{j\in\gamma_D(i)} \int_{\Gamma_{ij}} \sum_{s=1}^{d} R_s(u_h, \nabla u_h)\,(n_{ij})_s\,\varphi_h \,\mathrm{d}S \\
&+ \sum_{i\in I} \sum_{j\in\gamma_D(i)} \int_{\Gamma_{ij}} \sum_{s=1}^{d} R_s(u_h, \nabla \varphi_h)\,(n_{ij})_s\,u_h \,\mathrm{d}S
\end{aligned}
$$

$$
J_h(u_h,\varphi_h) = \sum_{i\in I} \sum_{j\in s(i)} \int_{\Gamma_{ij}} \sigma[u_h]\,[\varphi_h]\,\mathrm{d}S + \sum_{i\in I} \sum_{j\in\gamma_D(i)} \int_{\Gamma_{ij}} \sigma\,u_h\,\varphi_h\,\mathrm{d}S \tag{2.17}
$$

$$
\begin{aligned}
\ell_h(\varphi_h)\,(t) &= \int_\Omega g(t)\,\varphi_h\,\mathrm{d}x + \sum_{i\in I} \sum_{j\in\gamma_N(i)} \int_{\Gamma_{ij}} g_N\,\varphi_h\,\mathrm{d}S \\
&+ \sum_{i\in I} \sum_{j\in\gamma_D(i)} \int_{\Gamma_{ij}} \sum_{s=1}^{d} R_s(u, \nabla\varphi_h)\,(n_{ij})_s\,u_D(t)\,\mathrm{d}S \\
&+ \sum_{i\in I} \sum_{j\in\gamma_D(i)} \int_{\Gamma_{ij}} \sigma\,u_D(t)\,\varphi_h\,\mathrm{d}S,
\end{aligned} \tag{2.18}
$$

$$
(\alpha,\beta) = \int_\Omega \alpha\beta\,\mathrm{d}x. \tag{2.19}
$$

By $u(t)$ we denote the function on Ω such that $u(t)\,(x) = u(x,t)$, $x \in \Omega$. As $S_h \subset H^2(\Omega, \mathcal{T}_h)$ the previous forms have sense as well as for $u_h, \varphi_h \subset S_h$. Then we formulate the *discrete problem*: We define an approximate solution as a function u_h satisfying the conditions

(2.20) a) $u_h \in C^1([0,T], S_h)$,

b) $$\left(\frac{\partial u_h(t)}{\partial t}, \varphi_h\right) + b_h(u_h(t),\varphi_h) + a_h(u_h(t),\varphi_h) + J_h(u_h(t),\varphi_h) = \ell_h(\varphi_h)(t)$$
$$\forall\,\varphi_h \in S_h \quad \forall\,t \in (0,T),$$

c) $u_h(0) = u_h^0$,

where u_h^0 is an S_h-approximation of u^0 (e. g., L^2-projection).

We have carried out the semidiscretization in space (called the method of lines) leading to a system of ordinary differential equations. In practical computations, the full discretization is carried out. We can use, e. g. the explicit Euler or Runge–Kutta schemes. Semiimplicit or fully implicit time discretization leads to large nonlinear algebraic systems which must be solved iteratively. Moreover, the integrals are evaluated with the aid of quadrature formulae.

2.3 Numerical analysis

In [12] we consider a special case of (2.1) – (2.4) with

$$
\sum_{s=1}^{d} \frac{\partial R_s(u,\nabla u)}{\partial x_s} = \varepsilon\Delta u \tag{2.21}
$$

and

$$\partial\Omega_N = \emptyset, \tag{2.22}$$

where $\varepsilon > 0$ is a given constant which plays a role of viscosity. Using some assumption for triangulation and the numerical flux, we are able to prove the a priori error estimation for the error

$$e_h \equiv u_h - u, \tag{2.23}$$

where u is the exact solution of (2.1) – (2.4), (2.21), (2.22) and u_h is its approximate solution given by (2.20).

Assumptions (T): Let us consider a system $\{\mathcal{T}_h\}_{h\in(0,h_0)}$, $h_0 > 0$, of partitions of the domain Ω ($\mathcal{T}_h = \{K_i\}_{i\in I_h}$, $I_h \subset Z^+$) and assume that it has the following properties:

(T1) Each element $K \in \mathcal{T}_h$, $h \in (0, h_0)$ is *star-shaped* with respect to at least one point $x_K \in K$. We assume that

i) there exists a constant $\kappa > 0$ independent of K and h such that

$$\frac{\max_{x\in\partial K} |x - x_K|}{\min_{x\in\partial K} |x - x_K|} \le \kappa \quad \forall K \in \mathcal{T}_h,\ h \in (0, h_0), \tag{2.24}$$

ii) element K has piecewise smooth Lipschitz boundary and K can be divided into a finite number of simplex

$$\overline{K} = \bigcup_{S\in\mathcal{S}(K)} \overline{S}, \tag{2.25}$$

there exists a positive constant c_1 such that

$$\frac{h_S}{\rho_S} \le c_1 \quad \forall S \in \mathcal{S}(K) \qquad \text{(shape regularity)}, \tag{2.26}$$

where h_S is the diameter of S, ρ_S is the radius of the largest d-dimensional ball inscribed into S and moreover

$$0 < \frac{1}{\tilde{\kappa}} \le \frac{h_K}{h_S} \le \tilde{\kappa} < \infty \quad \forall S \in \mathcal{S}(K), \tag{2.27}$$

where h_K is the diameter of K and $\tilde{\kappa}$ is a constant independent of K and h.

(T2) There exists a constant $c_2 > 0$ such that

$$h_{K_i} \le c_2 d(\Gamma_{ij}), \quad i \in I, j \in S(i), h \in (0, h_0). \tag{2.28}$$

Assumptions (H):

1. $H(u,v,\boldsymbol{n})$ is defined in $\mathbb{R}^d \times \mathcal{S}_1$, where $\mathcal{S}_1 = \{\boldsymbol{n} \in \mathbb{R}^d; |\boldsymbol{n}| = 1\}$, and *Lipschitz-continuous* with respect to u, v:

$$|H(u,v,\boldsymbol{n}) - H(u^*,v^*,\boldsymbol{n})| \le c_3(|u-u^*| + |v-v|^*), \quad u,\ v,\ u^*,\ v^* \in \mathbb{R},\ \boldsymbol{n} \in \mathcal{S}_1. \tag{2.29}$$

2. $H(u,v,\boldsymbol{n})$ is *consistent*:

$$H(u,u,\boldsymbol{n}) = \sum_{s=1}^{d} f_s(u)\, n_s, \quad u \in \mathbb{R},\ \boldsymbol{n} = (n_1,\dots,n_d) \in \mathcal{S}_1. \tag{2.30}$$

3. $H(u,v,\boldsymbol{n})$ is *conservative*:

$$H(u,v,\boldsymbol{n}) = -H(v,u,-\boldsymbol{n}), \quad u,\ v \in \mathbb{R},\ \boldsymbol{n} \in \mathcal{S}_1. \tag{2.31}$$

Theorem 2.1 *Let assumptions* (T) *and* (H) *be satisfied. Let u be the exact strong solution of problem (2.1) – (2.4), (2.21), (2.22) satisfying*

$$u \in L^2(0,T;H^{p+1}(\Omega)), \quad \frac{\partial u}{\partial t} \in L^2(0,T;H^{p+1}(\Omega)), \tag{2.32}$$

where the integer number $p \ge 1$ is a given degree of approximation. Let u_h be the approximate solution defined by (2.20). Then the error $e_h = u_h - u$ satisfies the estimate

$$\begin{aligned} &\sup_{t\in[0,T]} \|e_h(t)\|^2_{L^2(\Omega)} + \varepsilon \int_0^T \left(|e_h(\vartheta)|^2_{H^1(\Omega,\mathcal{T}_h)} + J_h^\sigma(e_h(\vartheta),e_h(\vartheta)) \right) \mathrm{d}\vartheta \\ &\quad + C_1(1+\varepsilon) \int_0^T \left\{ \exp\left(C_1 \frac{1+\varepsilon}{\varepsilon}(T-\vartheta) \right) \right. \\ &\qquad \left. \times \left[\int_0^\vartheta \left(|e_h(\alpha)|^2_{H^1(\Omega,\mathcal{T}_h)} + J_h^\sigma(e_h(\alpha),e_h(\alpha)) \right) \mathrm{d}\alpha \right] \right\} \mathrm{d}\vartheta \\ &\le 2h^{2p} \left\{ \left(\frac{C_4(\varepsilon^2+h^2)}{\varepsilon} + c_2 + \varepsilon C_3 \right) \exp\left(C_1 \frac{1+\varepsilon}{\varepsilon} T \right) + C_2 \right\}, \end{aligned} \tag{2.33}$$

with constants $C_1,\dots,C_4 > 0$ independent of h and ε and c_2 is the constant from (2.28).

Proof: see [12]

Remark 2.2 This error estimate is not optimal as we have only first order of accuracy for piecewise linear approximation ($p = 1$). On the other hand, the numerical examples carried out in [12] confirm the second order of accuracy for $p = 1$.

3 System of the Navier-Stokes equations

In this section, our aim is to extend the approach explained above to the system of equations, particularly to the compressible Navier–Stokes equations. For simplicity, we shall consider a 2-dimensional problem, i.e., we assume that $d = 2$.

3.1 Governing equations

Let $\Omega \subset I\!R^2$ be a bounded domain and $T > 0$. We set $Q_T = \Omega \times (0, T)$ and by $\partial\Omega$ denote the boundary of Ω which consists of several disjoint parts. We distinguish inlet Γ_I, outlet Γ_O and impermeable walls Γ_W on $\partial\Omega$. The system of the compressible Navier-Stokes equations describing 2D viscous flow can be written in the dimensionless form

$$\frac{\partial \boldsymbol{w}}{\partial t} + \sum_{s=1}^{2} \frac{\partial \boldsymbol{f}_s(\boldsymbol{w})}{\partial x_s} = \frac{\partial \boldsymbol{R}_s(\boldsymbol{w}, \nabla \boldsymbol{w})}{\partial x_s} \quad \text{in } Q_T. \tag{3.1}$$

where

$$\boldsymbol{w} = (w_1, \ldots, w_4)^{\mathrm{T}} = (\rho,\, \rho v_1,\, \rho v_2,\, e)^{\mathrm{T}} \tag{3.2}$$

is the so-called *state vector*,

$$\begin{aligned} \boldsymbol{f}_s(\boldsymbol{w}) &= (f_s^1(\boldsymbol{w}), \ldots, f_s^4(\boldsymbol{w}))^{\mathrm{T}} \\ &= (\rho v_s,\, \rho v_s v_1 + \delta_{s1} p,\, \rho v_s v_2 + \delta_{s2} p,\, (e + p)\, v_s)^{\mathrm{T}},\ s = 1, 2, \end{aligned} \tag{3.3}$$

are the so-called *inviscid (Euler) fluxes* and

$$\begin{aligned} \boldsymbol{R}_s(\boldsymbol{w}, \nabla \boldsymbol{w}) &= (R_s^1(\boldsymbol{w}, \nabla \boldsymbol{w}), \ldots, R_s^4(\boldsymbol{w}, \nabla \boldsymbol{w}))^{\mathrm{T}} \\ &= \left(0,\, \tau_{s1}, \tau_{s2}, \sum_{k=1}^{2} \tau_{sk} v_k + \frac{\gamma}{Re\, Pr} \frac{\partial \theta}{\partial x_s}\right)^{\mathrm{T}},\ s = 1, 2, \end{aligned} \tag{3.4}$$

are the so-called *viscous fluxes*. We consider the Newtonian type of fluid, i. e., the stress tensor has the form

$$\tau_{sk} = \frac{1}{Re}\left[\left(\frac{\partial v_s}{\partial x_k} + \frac{\partial v_k}{\partial x_s}\right) - \frac{2}{3}\mathrm{div}(\boldsymbol{v})\, \delta_{sk}\right], \quad s, k = 1, 2. \tag{3.5}$$

We use the following notation: ρ – density, p – pressure, e – total energy, $\boldsymbol{v} = (v_1, v_2)$ – velocity, θ – absolute temperature, γ – Poisson adiabatic constant, Re – Reynolds number, Pr – Prandtl number.

In order to close the system we consider the following thermodynamical relations: the state equation for perfect gas and the relation for total energy

$$p = (\gamma - 1)\,(e - \rho|\boldsymbol{v}|^2/2), \quad e = c_V \rho\theta + \rho|\boldsymbol{v}|^2/2, \tag{3.6}$$

where c_V is the specific heat at constant volume which is equal to one in the dimensionless case. The system (3.1) – (3.6) is *hyperbolic-parabolic* type. It is equipped with the initial condition

$$\boldsymbol{w}(x, 0) = \boldsymbol{w}^0(x), \quad x \in \Omega, \tag{3.7}$$

and the following set of boundary conditions on appropriate parts of boundary:

$$\begin{aligned} &a) \quad \rho = \rho_D,\ \boldsymbol{v} = \boldsymbol{v}_D,\ \sum_{k=1}^{2}\left(\sum_{l=1}^{2} \tau_{lk} n_l\right) v_k + \frac{\gamma}{Re\, Pr}\frac{\partial \theta}{\partial \boldsymbol{n}} = 0 \quad \text{on } \Gamma_I, \\ &b) \quad \sum_{k=1}^{2} \tau_{sk} n_k = 0,\ s = 1, 2,\ \frac{\partial \theta}{\partial \boldsymbol{n}} = 0 \quad \text{on } \Gamma_O, \\ &c) \quad \boldsymbol{v} = 0,\ \frac{\partial \theta}{\partial \boldsymbol{n}} = 0 \quad \text{on } \Gamma_W, \end{aligned} \tag{3.8}$$

where ρ_D and $\boldsymbol{v}_D$ are given function and $\boldsymbol{n} = (n_1, n_2)$ is a unit outer normal to $\partial\Omega$. Another possibility is to replace the adiabatic boundary condition (3.8), c) by the

$$c')\ \boldsymbol{v} = 0,\ \theta = \theta_D \quad \text{on } \Gamma_W. \tag{3.9}$$

The question of a correct choice of the boundary conditions for the compressible Navier-Stokes equations is still open. Our choice is based on some heuristic considerations and various types of numerical experiments.

Putting $\boldsymbol{R}_s = 0,\ s = 1, 2$, in (3.1), we obtain the *Euler equations*

$$\frac{\partial \boldsymbol{w}}{\partial t} + \sum_{s=1}^{2} \frac{\partial \boldsymbol{f}_s(\boldsymbol{w})}{\partial x_s} = 0 \quad \text{in } Q_T, \tag{3.10}$$

which describe the motion of an inviscid compressible fluid. The system of the Euler equations is *hyperbolic*. For this case we replace the boundary conditions (3.8)–(3.9) by "inviscid" ones. We put $\boldsymbol{v} \cdot \boldsymbol{n} = 0$ on Γ_W and on Γ_I and Γ_O we consider the boundary conditions, which were derived for a linear system. It means that we prescribe m_n components of $\boldsymbol{w}$, and the other components are extrapolated from interior of Ω. Here m_n is the number of negative eigenvalues of the Jacobi matrix

$$\sum_{s=1}^{2} \frac{D\boldsymbol{f}_s(\boldsymbol{w})}{D\boldsymbol{w}} n_s. \tag{3.11}$$

For more detail see [16], [17], [27].

3.2 DG FE formulation

The extension of DG FE method from the scalar equation to the system of the Navier-Stokes equations is not quite straightforward. It is caused by the fact that the viscous terms $\boldsymbol{R}_s,\ s = 1, 2$ in (3.4) are more complicated than in the scalar case. In order to proceed in a similar way as in Section 2.2, we have to modify terms $\boldsymbol{R}_s,\ s = 1, 2$ so that they are linear with respect to $\nabla \boldsymbol{w}$.

Replacing the physical quantities ρ, $\boldsymbol{v}$ and θ by the components of the state vector $\boldsymbol{w}$ we have from (3.2) and (3.4)

$$\boldsymbol{R}_1(\boldsymbol{w}, \nabla \boldsymbol{w}) = \begin{pmatrix} 0 \\ \frac{2}{3}\frac{1}{Re}\left(2\frac{\partial}{\partial x_1}(\frac{w_2}{w_1}) - \frac{\partial}{\partial x_2}(\frac{w_3}{w_1})\right) \\ \frac{1}{Re}\left(\frac{\partial}{\partial x_1}(\frac{w_3}{w_1}) + \frac{\partial}{\partial x_2}(\frac{w_2}{w_1})\right) \\ \frac{w_2}{w_1}\boldsymbol{R}_1^{(2)} + \frac{w_3}{w_1}\boldsymbol{R}_1^{(3)} + \frac{\gamma}{Re\,Pr}\frac{\partial}{\partial x_1}\left(\frac{w_4}{w_1} - \frac{1}{2w_1^2}(w_2^2 + w_3^2)\right) \end{pmatrix}, \tag{3.12}$$

where $\boldsymbol{R}_1^{(2)}$ and $\boldsymbol{R}_1^{(3)}$ are the second and third component of $\boldsymbol{R}_1(\boldsymbol{w}, \nabla \boldsymbol{w})$, respectively, and

$$\boldsymbol{R}_2(\boldsymbol{w}, \nabla \boldsymbol{w}) = \begin{pmatrix} 0 \\ \frac{1}{Re}\left(\frac{\partial}{\partial x_1}(\frac{w_3}{w_1}) + \frac{\partial}{\partial x_2}(\frac{w_2}{w_1})\right) \\ \frac{2}{3}\frac{1}{Re}\left(2\frac{\partial}{\partial x_2}(\frac{w_3}{w_1}) - \frac{\partial}{\partial x_1}(\frac{w_2}{w_1})\right) \\ \frac{w_2}{w_1}\boldsymbol{R}_2^{(2)} + \frac{w_3}{w_1}\boldsymbol{R}_2^{(3)} + \frac{\gamma}{Re\,Pr}\frac{\partial}{\partial x_2}\left(\frac{w_4}{w_1} - \frac{1}{2w_1^2}(w_2^2 + w_3^3)\right) \end{pmatrix}, \tag{3.13}$$

where $\boldsymbol{R}_2^{(2)}$ and $\boldsymbol{R}_2^{(3)}$ are the second and third component of $\boldsymbol{R}_2(\boldsymbol{w}, \nabla \boldsymbol{w})$, respectively. Performing the chain rule in the terms $\boldsymbol{R}_s,\ s = 1, 2$ we have

$$\boldsymbol{R}_1(\boldsymbol{w}, \nabla \boldsymbol{w}) = \begin{pmatrix} 0 \\ \frac{2}{3}\frac{1}{Rew_1}\left[2\left(\frac{\partial w_2}{\partial x_1} - \frac{w_2}{w_1}\frac{\partial w_1}{\partial x_1}\right) - \left(\frac{\partial w_3}{\partial x_2} - \frac{w_3}{w_1}\frac{\partial w_1}{\partial x_2}\right)\right] \\ \frac{1}{Rew_1}\left[\left(\frac{\partial w_3}{\partial x_1} - \frac{w_3}{w_1}\frac{\partial w_1}{\partial x_1}\right) + \left(\frac{\partial w_2}{\partial x_2} - \frac{w_2}{w_1}\frac{\partial w_1}{\partial x_2}\right)\right] \\ \frac{w_2}{w_1}\boldsymbol{R}_1^{(2)} + \frac{w_3}{w_1}\boldsymbol{R}_1^{(3)} + \frac{\gamma}{Re\,Pr}\frac{1}{w_1}\times \\ \times\left[\frac{\partial w_4}{\partial x_1} - \frac{w_4}{w_1}\frac{\partial w_1}{\partial x_1} - \frac{1}{w_1}\left(w_2\frac{\partial w_2}{\partial x_1} + w_3\frac{\partial w_3}{\partial x_1}\right) + \frac{1}{w_1^2}(w_2^2 + w_3^2)\frac{\partial w_1}{\partial x_1})\right] \end{pmatrix}, \tag{3.14}$$

and

$$\boldsymbol{R}_2(\boldsymbol{w}, \nabla \boldsymbol{w}) = \begin{pmatrix} 0 \\ \frac{1}{Rew_1}\left[\left(\frac{\partial w_3}{\partial x_1} - \frac{w_3}{w_1}\frac{\partial w_1}{\partial x_1}\right) + \left(\frac{\partial w_2}{\partial x_2} - \frac{w_2}{w_1}\frac{\partial w_1}{\partial x_2}\right)\right] \\ \frac{2}{3}\frac{1}{Re\,w_1}\left[2\left(\frac{\partial w_3}{\partial x_2} - \frac{w_3}{w_1}\frac{\partial w_1}{\partial x_2}\right) - \left(\frac{\partial w_2}{\partial x_1} - \frac{w_2}{w_1}\frac{\partial w_1}{\partial x_1}\right)\right] \\ \frac{w_2}{w_1}\boldsymbol{R}_2^{(2)} + \frac{w_3}{w_1}\boldsymbol{R}_2^{(3)} + \frac{\gamma}{Re\,Pr}\frac{1}{w_1}\times \\ \times\left[\frac{\partial w_4}{\partial x_2} - \frac{w_4}{w_1}\frac{\partial w_1}{\partial x_2} - \frac{1}{w_1}\left(w_2\frac{\partial w_2}{\partial x_2} + w_3\frac{\partial w_3}{\partial x_2}\right) + \frac{1}{w_1^2}(w_2^2 + w_3^2)\frac{\partial w_1}{\partial x_2}\right] \end{pmatrix}. \tag{3.15}$$

For $\boldsymbol{\varphi} = (\varphi_1, \varphi_2, \varphi_3, \varphi_4)$ we define the forms

$$\boldsymbol{D}_1(\boldsymbol{w}, \nabla \boldsymbol{w}, \boldsymbol{\varphi}, \nabla \boldsymbol{\varphi}) \equiv \tag{3.16}$$
$$\begin{pmatrix} 0 \\ \frac{2}{3}\frac{1}{Rew_1}\left[2\left(\frac{\partial \varphi_2}{\partial x_1} - \frac{\varphi_2}{w_1}\frac{\partial w_1}{\partial x_1}\right) - \left(\frac{\partial \varphi_3}{\partial x_2} - \frac{\varphi_3}{w_1}\frac{\partial w_1}{\partial x_2}\right)\right] \\ \frac{1}{Rew_1}\left[\left(\frac{\partial \varphi_3}{\partial x_1} - \frac{\varphi_3}{w_1}\frac{\partial w_1}{\partial x_1}\right) + \left(\frac{\partial \varphi_2}{\partial x_2} - \frac{\varphi_2}{w_1}\frac{\partial w_1}{\partial x_2}\right)\right] \\ \frac{w_2}{w_1}\boldsymbol{D}_1^{(2)} + \frac{w_3}{w_1}\boldsymbol{D}_1^{(3)} + \frac{\gamma}{Re\,Pr}\frac{1}{w_1}\times \\ \times\left[\frac{\partial \varphi_4}{\partial x_1} - \frac{\varphi_4}{w_1}\frac{\partial w_1}{\partial x_1} - \frac{1}{w_1}\left(w_2\frac{\partial \varphi_2}{\partial x_1} + w_3\frac{\partial \varphi_3}{\partial x_1}\right) + \frac{1}{w_1^2}(w_2\varphi_2 + w_3\varphi_3)\frac{\partial w_1}{\partial x_1})\right] \end{pmatrix},$$

and

$$\boldsymbol{D}_2(\boldsymbol{w}, \nabla \boldsymbol{w}, \boldsymbol{\varphi}, \nabla \boldsymbol{\varphi}) \equiv \tag{3.17}$$
$$\begin{pmatrix} 0 \\ \frac{1}{Rew_1}\left[\left(\frac{\partial \varphi_3}{\partial x_1} - \frac{\varphi_3}{w_1}\frac{\partial w_1}{\partial x_1}\right) + \left(\frac{\partial \varphi_2}{\partial x_2} - \frac{\varphi_2}{w_1}\frac{\partial w_1}{\partial x_2}\right)\right] \\ \frac{2}{3}\frac{1}{Re\,w_1}\left[2\left(\frac{\partial \varphi_3}{\partial x_2} - \frac{\varphi_3}{w_1}\frac{\partial w_1}{\partial x_2}\right) - \left(\frac{\partial \varphi_2}{\partial x_1} - \frac{\varphi_2}{w_1}\frac{\partial w_1}{\partial x_1}\right)\right] \\ \frac{w_2}{w_1}\boldsymbol{D}_2^{(2)} + \frac{w_3}{w_1}\boldsymbol{D}_2^{(3)} + \frac{\gamma}{Re\,Pr}\frac{1}{w_1}\times \\ \times\left[\frac{\partial \varphi_4}{\partial x_2} - \frac{\varphi_4}{w_1}\frac{\partial w_1}{\partial x_2} - \frac{1}{w_1}\left(w_2\frac{\partial \varphi_2}{\partial x_2} + w_3\frac{\partial \varphi_3}{\partial x_2}\right) + \frac{1}{w_1^2}(w_2\varphi_2 + w_3\varphi_2)\frac{\partial w_1}{\partial x_2}\right] \end{pmatrix}.$$

where $\boldsymbol{D}_s^{(2)},\ \boldsymbol{D}_s^{(3)},\ s=1,2$ are the second and third components of $\boldsymbol{D}_s(\boldsymbol{w},\nabla\boldsymbol{w})$, respectively. Obviously

$$\boldsymbol{D}_s(\boldsymbol{w},\nabla\boldsymbol{w},\boldsymbol{w},\nabla\boldsymbol{w}) = \boldsymbol{R}_s(\boldsymbol{w},\nabla\boldsymbol{w}), \qquad s=1,2 \tag{3.18}$$

and the forms $\boldsymbol{D}_s(\boldsymbol{w},\nabla\boldsymbol{w},\boldsymbol{\varphi},\nabla\boldsymbol{\varphi}),\ s=1,2$ are linear with respect $\boldsymbol{\varphi}$ and $\nabla\boldsymbol{\varphi}$ and therefore they satisfy the assumption of linearity as the forms $R_s(u,\alpha),\ s=1,2$ from the scalar case. There are several possibilities how to define the forms $\boldsymbol{D}_s,\ s=1,2$. Based on a wide range of numerical experiments, the presented possibility (3.16)–(3.17) seems to us the best one. On the other hand, in the absence of a theoretical background, this question is still open.

In order to derive the weak formulation, we multiply (3.1) (where we replace the terms $\boldsymbol{R}_s$ by the terms $\boldsymbol{D}_s,\ s=1,2$) by a function $\boldsymbol{\varphi}\in\left[H^k(\Omega,\mathcal{T}_h)\right]^4$ and integrate over an element $K_i,\ i\in I$. Further we sum over all K_i and add similar stabilization terms as for the scalar equation. Taking into account the boundary condition (3.8), we obtain the integral identity (compare with (2.11))

$$\begin{aligned}
&\frac{\mathrm{d}}{\mathrm{d}t}\sum_{K_i\in\mathcal{T}_h}\int_{K_i}\boldsymbol{w}\cdot\boldsymbol{\varphi}\,\mathrm{d}x = \\
&+\sum_{K_i\in\mathcal{T}_h}\int_{K_i}\sum_{s=1}^{2}\boldsymbol{f}_s(\boldsymbol{w})\cdot\frac{\partial\boldsymbol{\varphi}}{\partial x_s}\,\mathrm{d}x \\
&-\sum_{K_i\in\mathcal{T}_h}\sum_{j\in S(i)}\int_{\Gamma_{ij}}\sum_{s=1}^{2}\boldsymbol{f}_s(\boldsymbol{w})\cdot\boldsymbol{\varphi}\,(n_{ij})_s\,\mathrm{d}S \\
&-\sum_{K_i\in\mathcal{T}_h}\int_{K_i}\sum_{s=1}^{2}\boldsymbol{D}_s(\boldsymbol{w},\nabla\boldsymbol{w},\boldsymbol{w},\nabla\boldsymbol{w})\cdot\frac{\partial\boldsymbol{\varphi}}{\partial x_s}\,\mathrm{d}x \\
&+\sum_{K_i\in\mathcal{T}_h}\sum_{\substack{j\in s(i)\\ j<i}}\int_{\Gamma_{ij}}\sum_{s=1}^{2}\langle\boldsymbol{D}_s(\boldsymbol{w},\nabla\boldsymbol{w},\boldsymbol{w},\nabla\boldsymbol{w})\rangle\,(n_{ij})_s\cdot[\boldsymbol{\varphi}]\,\mathrm{d}S \\
&-\sum_{K_i\in\mathcal{T}_h}\sum_{\substack{j\in s(i)\\ j<i}}\int_{\Gamma_{ij}}\sum_{s=1}^{2}\langle\boldsymbol{D}_s(\boldsymbol{w},\nabla\boldsymbol{w},\boldsymbol{\varphi},\nabla\boldsymbol{\varphi})\rangle\,(n_{ij})_s\cdot[\boldsymbol{w}]\,\mathrm{d}S \\
&+\sum_{K_i\in\mathcal{T}_h}\sum_{j\in\gamma_D(i)}\int_{\Gamma_{ij}}\sum_{s=1}^{2}\boldsymbol{D}_s(\boldsymbol{w},\nabla\boldsymbol{w},\boldsymbol{w},\nabla\boldsymbol{w})\,(n_{ij})_s\cdot\boldsymbol{\varphi}\,\mathrm{d}S \\
&-\sum_{K_i\in\mathcal{T}_h}\sum_{j\in\gamma_D(i)}\int_{\Gamma_{ij}}\sum_{s=1}^{2}\boldsymbol{D}_s(\boldsymbol{w},\nabla\boldsymbol{w},\boldsymbol{\varphi},\nabla\boldsymbol{\varphi})\,(n_{ij})_s\cdot(\boldsymbol{w}-\boldsymbol{w}_B)\,\mathrm{d}S \\
&-\sum_{K_i\in\mathcal{T}_h}\sum_{\substack{j\in s(i)\\ j<i}}\int_{\Gamma_{ij}}\sigma[\boldsymbol{w}]\cdot[\boldsymbol{\varphi}]\,\mathrm{d}S \\
&-\sum_{K_i\in\mathcal{T}_h}\sum_{j\in\gamma_D(i)}\int_{\Gamma_{ij}}\sigma(\boldsymbol{w}-\boldsymbol{w}_B)\cdot\boldsymbol{\varphi}\,\mathrm{d}S
\end{aligned} \tag{3.19}$$

where $\sigma=(|\Gamma_{ij}|\,Re)^{-1}$. The set $\gamma_D(i)$ contains edges where the Dirichlet boundary

condition is given for at least one component of $\boldsymbol{w} = (w_1, \ldots, w_4)$, i.e., edges lying on Γ_I or Γ_W. We prescribe the boundary state $\boldsymbol{w}_B = ((w_B)_1, \ldots, (w_B)_4)$ by

$$(w_B)_r = \begin{cases} (w_D)_r & \text{if } w_r \text{ is prescribed on } \partial\Omega \\ w_r & \text{otherwise,} \end{cases}, \ r = 1, \ldots, 4. \tag{3.20}$$

In particular, for the case (3.8) a)–c) we have

$$\begin{aligned} \boldsymbol{w}_B &= (\rho|_{\Gamma_W}, 0, 0, \rho|_{\Gamma_W}\theta|_{\Gamma_W}) \text{ on } \Gamma_W, \\ \boldsymbol{w}_B &= (\rho_D, \rho_D(\boldsymbol{v}_D)_1, \rho_D(\boldsymbol{v}_D)_2, \rho|_{\Gamma_I}\theta|_{\Gamma_I} + \frac{1}{2}\rho_D|\boldsymbol{v}_D|^2) \text{ on } \Gamma_I, \end{aligned} \tag{3.21}$$

and for the case (3.8) a)–b), (3.9) c')

$$\begin{aligned} \boldsymbol{w}_B &= (\rho|_{\Gamma_W}, 0, 0, \rho|_{\Gamma_W}\theta_D) \text{ on } \Gamma_W, \\ \boldsymbol{w}_B &= (\rho_D, \rho_D(\boldsymbol{v}_D)_1, \rho_D(\boldsymbol{v}_D)_2, \rho|_{\Gamma_I}\theta|_{\Gamma_I} + \frac{1}{2}\rho_D|\boldsymbol{v}_D|^2) \text{ on } \Gamma_I, \end{aligned} \tag{3.22}$$

where $\rho_D, \boldsymbol{v}_D$ and θ_D are given functions from the boundary conditions (3.8)–(3.9) and $\rho|_\Gamma$ and $\theta|_\Gamma$ are the values of density and temperature extrapolated from in interior of Ω on the appropriate boundary part Γ, respectively.

The relation (3.19) represents a weak form of the Navier-Stokes equations in the sense of the broken Sobolev space $[H^1(\Omega, \mathcal{T}_h)]^4$.

3.3 Numerical solution

In order to proceed from (3.19) to the numerical scheme for the system of equations, we use the same strategy as for the scalar equation in Section 2.2. By $\boldsymbol{w}(t)$ we denote the function on Ω such that $\boldsymbol{w}(t)\,(x) = \boldsymbol{w}(x,t)$, $x \in \Omega$. The relation (3.19) has sense for $\boldsymbol{w}(t), \boldsymbol{\varphi} \in [S_h]^4$, $t \in (0,T)$. In the following we present the schemes for the numerical solutions of inviscid or viscous flow described by systems (3.10) or (3.1), respectively.

3.3.1 Inviscid case

The second term on the right–hand side of (3.19) (boundary integral for inviscid fluxes) is approximated by the approach common in the finite volume method. We put

$$\int_{\Gamma_{ij}} \sum_{s=1}^{2} \boldsymbol{f}_s(\boldsymbol{w}(t))\, n_s \boldsymbol{\varphi}\, \mathrm{d}S \approx \int_{\Gamma_{ij}} \boldsymbol{H}(\boldsymbol{w}|_{\Gamma_{ij}}(x,t), \boldsymbol{w}|_{\Gamma_{ji}}(x,t), \boldsymbol{n}_{ij(x)})\boldsymbol{\varphi}|_{\Gamma_{ij}}(x)\mathrm{d}S, \tag{3.23}$$

where $\boldsymbol{H}$ is *the numerical flux*, $\boldsymbol{w}|_{\Gamma_{ij}}(x,\cdot)$ and $\boldsymbol{w}|_{\Gamma_{ji}}(x,\cdot)$ are the values of $\boldsymbol{w}$ at $x \in \Gamma_{ij}$ considered from interior and exterior of K_i, respectively. We use the numerical flux based on the direct solution of the local Riemann problem, see [14, 27].

For $\boldsymbol{w}_h(t), \boldsymbol{\varphi}_h \in [S_h]^4$ we introduce the forms

$$(\boldsymbol{w}_h, \boldsymbol{\varphi}_h) = \int_\Omega \boldsymbol{w}_h(x,t) \cdot \boldsymbol{\varphi}_h(x)\, \mathrm{d}x, \tag{3.24}$$

$$\begin{aligned}\boldsymbol{B}_h(\boldsymbol{w}_h,\boldsymbol{\varphi}_h) &= -\sum_{K_i\in\mathcal{T}_h}\int_{K_i}\sum_{s=1}^{2}\boldsymbol{f}_s(\boldsymbol{w}_h(x,t))\cdot\frac{\partial\boldsymbol{\varphi}_h(x)}{\partial x_s}\,\mathrm{d}x\\ &+ \sum_{K_i\in\mathcal{T}_h}\sum_{j\in S(i)}\int_{\Gamma_{ij}}\boldsymbol{H}(\boldsymbol{w}_h|_{\Gamma_{ij}}(x,t),\boldsymbol{w}_h|_{\Gamma_{ji}}(x,t),\boldsymbol{n}_{ij}(x))\cdot\boldsymbol{\varphi}_h(x)\mathrm{d}S.\end{aligned}$$

It is necessary define the meaning of $\boldsymbol{w}_h|_{\Gamma_{ji}}$ for $j\in\gamma(i)$. We use the "inviscid" boundary condition mentioned in Section 3.1. We say that $\boldsymbol{w}_h$ is the *approximate solution* of the system of the Euler equations (3.10), if it satisfies the conditions

$$\begin{aligned}&\text{(3.25) a)}\quad \boldsymbol{w}_h\in C^1([0,T],[S_h]^4),\\ &\text{b)}\quad \frac{\mathrm{d}}{\mathrm{d}t}(\boldsymbol{w}_h(t),\boldsymbol{\varphi}_h)+\boldsymbol{B}_h(\boldsymbol{w}_h(t),\boldsymbol{\varphi}_h)=0\quad\forall\,\boldsymbol{\varphi}_h\in[S_h]^4\ \forall\,t\in(0,T),\\ &\text{c)}\quad \boldsymbol{w}_h(0)=\boldsymbol{w}_h^0.\end{aligned}$$

3.3.2 Viscous case

Let $\boldsymbol{B}_h$ be the form introduced in (3.24). We denote by $\boldsymbol{A}_h(\boldsymbol{w},\boldsymbol{\varphi})$ the diffusive and stabilization part of the right hand side of (3.19), i.e., all terms where appears the terms $\boldsymbol{D}_s$ or σ. The form $\boldsymbol{A}_h(\cdot,\cdot)$ has sense for $\boldsymbol{w}_h(t),\boldsymbol{\varphi}_h\in[S_h]^4$. We say that $\boldsymbol{w}_h$ is an *approximate solution* of (3.19), if it satisfies the conditions

$$\begin{aligned}&\text{(3.26)}\quad \text{a)}\quad \boldsymbol{w}_h\in C^1([0,T],[S_h]^4),\\ &\text{b)}\quad \frac{\mathrm{d}}{\mathrm{d}t}(\boldsymbol{w}_h(t),\boldsymbol{\varphi}_h)=\boldsymbol{A}_h(\boldsymbol{w}_h(t),\boldsymbol{\varphi}_h)-\boldsymbol{B}_h(\boldsymbol{w}_h(t),\boldsymbol{\varphi}_h),\\ &\qquad\qquad\qquad\qquad\qquad\qquad\forall\,\boldsymbol{\varphi}_h\in[S_h]^4\ \forall\,t\in(0,T),\\ &\text{c)}\quad \boldsymbol{w}_h(0)=\boldsymbol{w}_h^0.\end{aligned}$$

The relations (3.25) and (3.26) are the basic numerical schemes for the solution of the Euler and the Navier-Stokes equations, respectively, with the aid of DG FE method. They represent a system of ordinary differential equations which can be solved by a suitable numerical method.

Let us remark that the scheme (3.25) does not contain any stabilization terms. Moreover, (3.25) is a special case of (3.26), with $\boldsymbol{A}_h=0$.

3.4 Implementation

The computation of the approximate solution was realized over regular triangular grids with the aid of piecewise linear approximations, i. e., with $p=1$ in (2.9). We use the basis of $S_h:=S^{1,-1}$ whose components are piecewise linear functions associated with midpoints of sides of triangles:

$$\text{(3.27)}\qquad \{\phi_{ij}\in S_h;\phi_{ij}(Q_{kl})=\delta_{ik}\delta_{jl},\ j\in S(i),\ l\in S(k),\ i,k\in I\}\,,$$

where Q_{kl} is the midpoint of Γ_{kl}. This choice leads to a diagonal mass matrix in (3.25), b) and (3.26), b). For the evaluation of boundary integrals in (3.19) we use the two point Gauss quadrature rule

$$\text{(3.28)}\qquad \int_{-1}^{1}g(t)\,\mathrm{d}t\approx g\left(-\frac{1}{\sqrt{3}}\right)+g\left(\frac{1}{\sqrt{3}}\right),$$

which is exact for polynomials of the third degree. The volume integrals in (3.19) are evaluated by the three point integration rule

$$\int_{K_i} g(x)\,\mathrm{d}x \approx |K_i|\frac{1}{3}\sum_{j\in S(i)} g(Q_{ij}), \tag{3.29}$$

which is exact for second degree polynomials. The systems of ordinary differential equations (3.25) and (3.26) are solved by the forward Euler method. The use of the explicit scheme requires a restriction on a time step. Based on heuristic consideration and a number of numerical experiments we use the stability condition in the form

$$\Delta t = \frac{1}{3}\,CFL \min\left(\frac{1}{2}\max_{\substack{K_i\in T_h\\ j\in S(i)}}\left(\frac{|K_i|}{\lambda_{ij}|\Gamma_{ij}|}\right), \frac{1}{8}\max_{K_i\in T_h}\frac{Re}{|K_i|}\right), \tag{3.30}$$

where we put usually $CFL = 0.4$ and λ_{ij} is the maximal eigenvalue of the Jacobi matrix (3.11) evaluated over Γ_{ij}.

4 Limiting

The solution of problems with zero or small viscosity (high Reynolds number) contains discontinuities or steep gradients of computed quantities, respectively. Their numerical approximations obtained by (3.25) and/or (3.26) usually contain spurious oscillations. In order to avoid these unphysical phenomena, we developed an indicator which seeks elements $K \in \mathcal{T}_h$ on which the approximate solution has large interelement jumps, representing discontinuities. On these elements the order limiting is applied, switching from a piecewise linear approximation to a piecewise constant approximation.

Numerical experiments carried out in [15] for scalar conservation laws show that the interelement jumps in the approximate solution are of the order $O(1)$ in vicinity of discontinuities, whereas $O(h^2)$ in the areas where the solution is regular. Therefore, the interelement jumps of order $O(h^\alpha)$ with $\alpha \in (0,2)$ represent a natural interface between "smooth" and "discontinuous" parts of the solution. In [15] we showed that for the case of a scalar equation, it is suitable to measure the magnitude of interelement jumps of the numerical solution u_h in the integral form by

$$\int_{\partial K_i} [u_h]^2\,\mathrm{d}S, \quad K_i \in \mathcal{T}_h, \tag{4.1}$$

where $[u_h]$ denotes the jump of u_h on sides of K_i.

Here we extend the control of jumps also to the system of the Euler and the Navier-Stokes equations. In order to detect discontinuities of the solutions (shock waves, contact discontinuities), it is suitable to measure the jumps of the density. Based on presented results and numerical experiments we define the *jump indicator*

$$g(i) = \frac{\int_{\partial K_i}[\rho]^2\,\mathrm{d}S}{h_i|K_i|^{3/4}}, \tag{4.2}$$

which is of order $O(1)$, if $[\rho] = O(h^{3/4})$.

Let us return to schemes (3.25) and (3.26). We carry out the discretization in time by the forward Euler method. To this end, we consider a partition $0 = t_0 < t_1 < t_2 < \dots$ of the time interval $(0, T)$ and set $\tau_k = t_{k+1} - t_k$. Then the *full discrete problems* read: for each $k \geq 0$ find $\boldsymbol{w}_h^{k+1} \in [S_h]^4$ such that

$$(\boldsymbol{w}_h^{k+1}, \boldsymbol{\varphi}_h) = (\boldsymbol{w}_h^k, \boldsymbol{\varphi}_h) - \tau_k \, \boldsymbol{B}_h(\boldsymbol{w}_h^k, \boldsymbol{\varphi}_h) \quad \forall\, \boldsymbol{\varphi}_h \in S_h, \tag{4.3}$$

Euler equations

$$(\boldsymbol{w}_h^{k+1}, \boldsymbol{\varphi}_h) = (\boldsymbol{w}_h^k, \boldsymbol{\varphi}_h) + \tau_k \left(\boldsymbol{A}_h(\boldsymbol{w}_h^k, \boldsymbol{\varphi}_h) - \boldsymbol{B}_h(\boldsymbol{w}_h^k, \boldsymbol{\varphi}_h) \right) \quad \forall\, \boldsymbol{\varphi}_h \in S_h. \tag{4.4}$$

Navier-Stokes equations

Now, for each time step we apply the limitation procedure in the following way. The schemes (4.3) – (4.4) are replaced by

$$(\boldsymbol{w}_h^{k+1}, \boldsymbol{\varphi}_h) = (\bar{\boldsymbol{w}}_h^k, \boldsymbol{\varphi}_h) - \tau_k \, \boldsymbol{B}_h(\bar{\boldsymbol{w}}_h^k, \boldsymbol{\varphi}_h) \quad \forall\, \boldsymbol{\varphi}_h \in S_h, \tag{4.5}$$

Euler equations

$$(\boldsymbol{w}_h^{k+1}, \boldsymbol{\varphi}_h) = (\bar{\boldsymbol{w}}_h^k, \boldsymbol{\varphi}_h) + \tau_k \left(\boldsymbol{A}_h(\boldsymbol{w}_h^k, \boldsymbol{\varphi}_h) - \boldsymbol{B}_h(\bar{\boldsymbol{w}}_h^k, \boldsymbol{\varphi}_h) \right) \quad \forall\, \boldsymbol{\varphi}_h \in S_h, \tag{4.6}$$

Navier-Stokes equations

where

$$\bar{\boldsymbol{w}}_h^k|_{K_i} := \begin{cases} \pi_0 \boldsymbol{w}_h^k|_{K_i} & \text{if } g(i) > 1, \\ \boldsymbol{w}_h^k|_{K_i} & \text{otherwise,} \end{cases} \qquad K_i \in \mathcal{T}_h, \tag{4.7}$$

and

$$\pi_0 \boldsymbol{w}_h|_{K_i} \in P_0(K_i), \ \pi_0 \boldsymbol{w}_h|_{K_i} = \frac{1}{K_i} \int_{K_i} \boldsymbol{w}_h \, \mathrm{d}x. \tag{4.8}$$

Let as recall that the limitation in (4.6) is not performed in the diffusive form $\boldsymbol{A}_h(\cdot, \cdot)$. Numerical examples confirm the high efficiency of the limiting procedure (4.2), (4.5) – (4.8). Namely, Figures 5, 7 and 9 in Section 6 show the capturing of the discontinuity (shock wave) without any unphysical oscillation.

5 Superparametric FE on a nonpolygonal boundary

Numerical experiments show that in some cases the DG FE method does not give good resolution in a neighbourhood of nonpolygonal parts of the boundary $\partial\Omega$, see Example 1 in Section 6. In order to get a satisfactory solution, it is necessary to use superparametric finite elements or a suitable numerical integration, see [4] and [24]. We use the first approach.

Let $\{K_i, \ i \in I_c, \ I_c \subset I\}$ be a set of triangles adjacent to a nonpolygonal part of $\partial\Omega$, see Figure 1. Let $P_i^k, \ k = 0, 1, 2$ be the vertices of K_i and moreover $P_i^k \in \partial\Omega$ for $k = 1, 2$ and $i \in I_c$. We suppose that the centre $P_i^{12} \in \partial\Omega$ of the curved side with endpoints P_i^1, P_i^2 is close to the centre of the straight segment $P_i^1 P_i^2$, see Figure 1.

Then there exists a unique *bilinear* mapping $F_i : \hat{K} \to K_i, F_i = (F_i^1, F_i^2)$, such that

$$\begin{aligned} F_i(\hat{P}^k) &= P_i^k, \quad k = 0, 1, 2, \\ F_i(\hat{P}^{12}) &= P_i^{12}, \end{aligned} \tag{5.1}$$

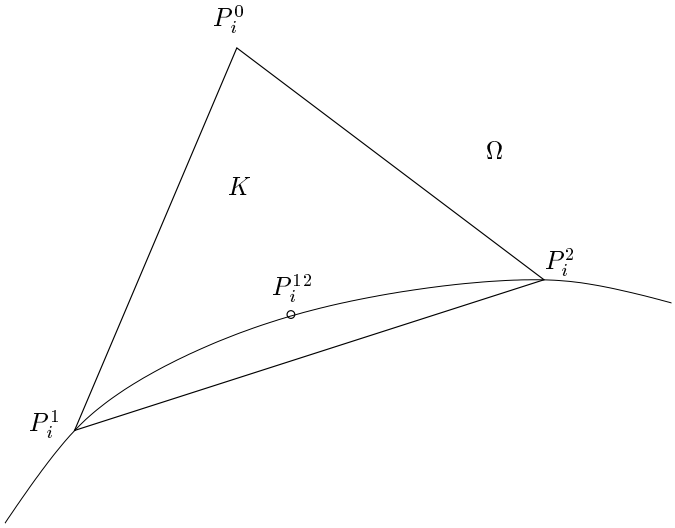

Figure 1: Triangle $K_i,\ i \in I_c$ lying on a nonpolygonal part of $\partial\Omega$

where $\hat{K}$ is a reference triangle with vertices

$$\hat{P}^0 = [0;0], \quad \hat{P}^1 = [1;0], \quad \hat{P}^2 = [0;1] \tag{5.2}$$

and

$$\hat{P}^{12} = [1/2;1/2], \tag{5.3}$$

see Figure 2.

Then the triangles $K_i,\ i \in I_c$, are replaced by the "curved triangles" defined by

$$\bar{K}_i = F_i(\hat{K}). \tag{5.4}$$

The "curved triangle" $\bar{K}_i$ is a plane figure having two straight sides and one curved side, see Figure 2. If $i \notin I_c$ then F_i is a linear mapping and, therefore, $\bar{K}_i = K_i$.

Now we describe how to evaluate the volume and boundary integrals over the elements $\bar{K}_i,\ i \in I_c$ and their sides Γ_{ij}. We denote by

$$J_{F_i}(\hat{x}) \equiv \frac{D\,F_i}{D\,\hat{x}}(\hat{x}), \quad \hat{x} \in \hat{K}, \tag{5.5}$$

the Jacobi matrix of the mapping F_i. Since F_i is bilinear, we easily find that $\det J_{F_i}$ is a linear function of the variable $\hat{x}$. The components of the vector valued test functions $\boldsymbol{\varphi}_h$ from (3.25) and (3.26) are defined on the boundary elements $\bar{K}_i$ with the aid of the mapping F_i. Denoting by $\hat{\varphi}$ any linear function on the reference element $\hat{K}$, we set

$$\varphi_h(x) = \hat{\varphi}(F_i^{-1}(x)), \quad x \in K_i. \tag{5.6}$$

These functions form the components of the test functions from the discrete problem. Then the terms in (4.5) and (4.5) have modified form. We present it only for inviscid

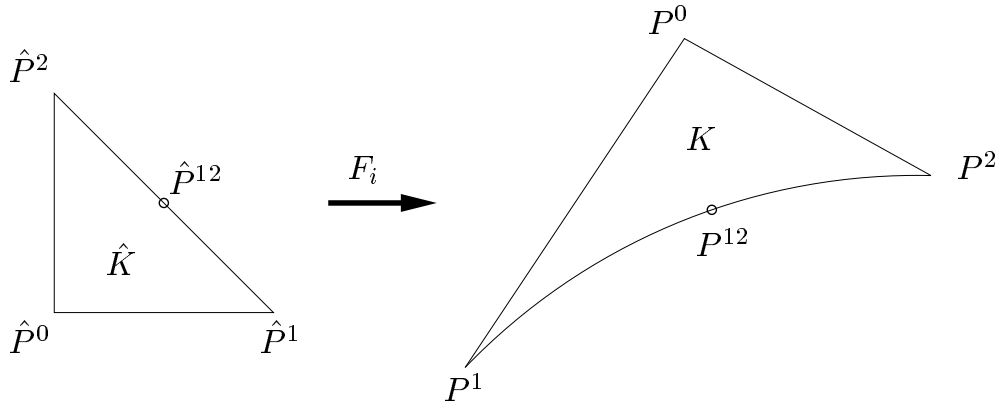

Figure 2: Bilinear mapping $F_i : \hat{K} \to K_i$

scheme (4.5), the modification of integrals of the form $\boldsymbol{A}_h(\cdot,\cdot)$ is very similar as for $\boldsymbol{B}_h(\cdot,\cdot)$.

The first form in (3.24) is expressed as

$$\int_{\bar{K}_i} \boldsymbol{w}_h(x,t)\cdot\boldsymbol{\varphi}_h(x)\,\mathrm{d}x = \int_{\hat{K}} \det J_{F_i}(\hat{x})\hat{\boldsymbol{w}}_i(\hat{x},t)\cdot\boldsymbol{\varphi}_h(\hat{x})\,\mathrm{d}\hat{x}, \quad i\in I, \tag{5.7}$$

where $\hat{\boldsymbol{w}}_i(\hat{x},t) = \boldsymbol{w}_h(F_i^{-1}(x),t)$.

Moreover, the volume integral in the form $\boldsymbol{B}_h$ in (3.24) is computed with the aid of

$$\begin{aligned}&\int_{\bar{K}_i}\sum_{s=1}^{2}\boldsymbol{f}_s(\boldsymbol{w}_h(x,t))\cdot\frac{\partial\boldsymbol{\varphi}_h(x)}{\partial x_s}\,\mathrm{d}x \\ &= \int_{\hat{K}}\det J_{F_i}(\hat{x})\sum_{s=1}^{2}\boldsymbol{f}_s(\hat{\boldsymbol{w}}_i(\hat{x},t))\cdot\sum_{j=1}^{2}\frac{\partial\hat{\boldsymbol{\varphi}}}{\partial\hat{x}_j}\frac{\partial(F_i^{-1})^j(F_i(\hat{x}))}{\partial x_s}\,\mathrm{d}\hat{x}, \quad i\in I,\end{aligned} \tag{5.8}$$

where $(F_i^{-1})^j$ denotes the j-th component of the inverse mapping F_i^{-1}. In order to compute the inverse mapping F_i^{-1} we use the following relation written in matrix form:

$$\frac{D\,F_i^{-1}}{Dx}(F_i(\hat{x})) = \left[\frac{D\,F_i}{D\hat{x}}(\hat{x})\right]^{-1} \tag{5.9}$$

following from the identity $x = F_i(F_i^{-1}(x))$. The computation of the inverse matrix in (5.9) is simpler than the evaluation of F_i^{-1}.

Further, the boundary integral over a side $\Gamma_{ij}\subset\bar{K}_i$ in the form $\boldsymbol{B}_h$ in (3.24) is computed with the aid of

$$\begin{aligned}&\int_{\Gamma_{ij}}\boldsymbol{H}(\boldsymbol{w}_h^+(x,t),\boldsymbol{w}_h^-(x,t),\boldsymbol{n}_{ij})\cdot\boldsymbol{\varphi}_h(x)\,\mathrm{d}S \\ &= \int_{\hat{\Gamma}}\boldsymbol{H}(\boldsymbol{w}_h^+(F_i(\hat{x}),t),\boldsymbol{w}_h^-(F_i(\hat{x}),t),\hat{\boldsymbol{n}}_{ij}(\hat{x}))\cdot\hat{\boldsymbol{\varphi}}(\hat{x})\beta(\hat{x})\,\mathrm{d}\hat{S},\end{aligned} \tag{5.10}$$

where $\hat{\Gamma}$ is the side of $\hat{K}$ corresponding to the curved side of $\bar{K}_i$ in the mapping $F_i = (F_i^1, F_i^2)$ and $\boldsymbol{w}_h^{\pm}(x,t) = \boldsymbol{w}_h^{\pm}(F_i(\hat{x}),t)$. The function $\beta(\hat{x})$ represents a boundary increase for boundary integral in a suitable parametrization $x_1 = x_1(s), x_2 = x_2(s)$:

$$\int_\Gamma u(x_1,x_2)\,\mathrm{d}S = \int_{s_1}^{s_2} u(x_1(s),x_2(s))\sqrt{(x_1'(s))^2+(x_2'(s))^2}\,\mathrm{d}s = \tag{5.11}$$

$$= \int_{\hat{s}_1}^{\hat{s}_2} u(F_i^1(\hat{x}_1(\hat{s}),\hat{x}_2(\hat{s})),F_i^2(\hat{x}_1(\hat{s}),\hat{x}_2(\hat{s})))\beta(\hat{x}_1(\hat{s}),\hat{x}_2(\hat{s}))\mathrm{d}\hat{s}.$$

Finally, the integrals over the reference triangle $\hat{K}$ and over the reference edge $\hat{\Gamma}$ in (5.7), (5.8) and (5.10) are evaluated with the aid of (3.29) and (3.28), respectively. Such approach essentially improves the quality of the solution in s neighbourhood of a nonpolygonal part of the boundary as is shown in Section 6, Figures 4 and 5.

6 Numerical examples

We present several examples representing the use of DG FE method for the numerical simulation of compressible flows. We applied the time stabilization method ($t \to \infty$) in order to obtain a steady state solution. The used triangular grid were obtained by the anisotropic mesh adaptation method (AMA), see [10], [11].

Examples 1 The first set of numerical examples deal with inviscid transonic flow through the GAMM channel. The inlet Mach number = 0.67 produces a shock wave. We demonstrate the influence of the use of the superparametric finite elements for triangles lying at the nonpolygonal part of $\partial\Omega$ explained in Section 5. The computations were performed on a very coarse grid from Figure 3 having 784 triangles where such an effect is better observed. Figures 4 and 5 show the distribution of the density in the computational domain and along the lower wall obtained by scheme (4.5) without and with the use of the bilinear mapping, respectively.

Figure 7 shows the distribution of the density in Ω and along the lower wall obtained with the aid of the bilinear mapping on the refined mesh shown in Figure 6. Here a very sharp capturing of the shock wave and the Zierep singularity are observed.

Example 2 Next example is the the simulation of inviscid around the profile NACA0012 with inlet Mach number $M_{\mathrm{in}} = 0.8$ and zero angle of attack. Figure 8 shows the the final mesh (obtained by AMA) and the isolines of the Mach number of this example. As we use a discontinuous approximation then the isolines are discontinuous of course. Figure 9 shows the distribution of Mach number and the pressure coefficient c_p around profile. We put

$$c_p = -\frac{p-p_\infty}{\frac{1}{2}\rho_\infty|\boldsymbol{v}_\infty|^2}, \tag{6.1}$$

where ρ_∞, $\boldsymbol{v}_\infty$ and p_∞ are the value of density, velocity and pressure at infinity, respectively. Although the used grid is relatively coarse (number of triangles

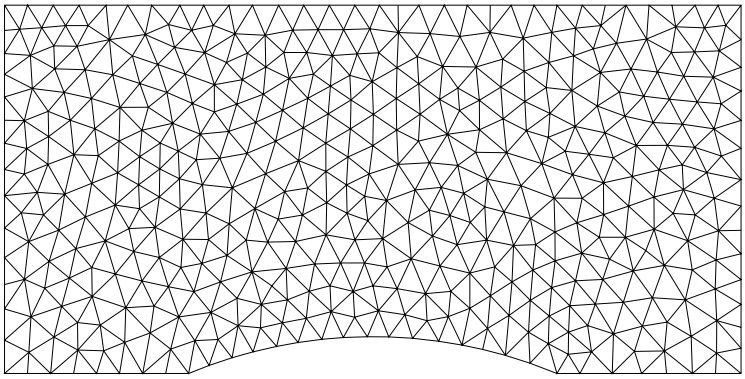

Figure 3: Coarse triangular mesh (784 triangles)

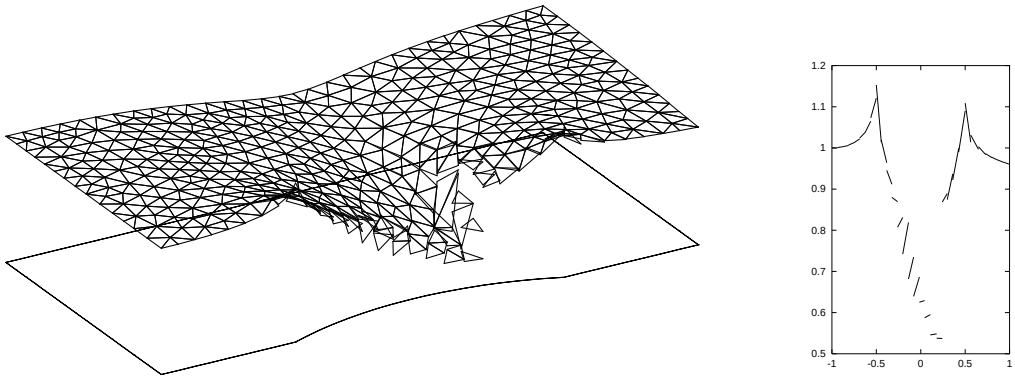

Figure 4: Distribution of the density in the computational domain (left) and along the lower wall (right) without the use of the superparametric FE at $\partial\Omega$

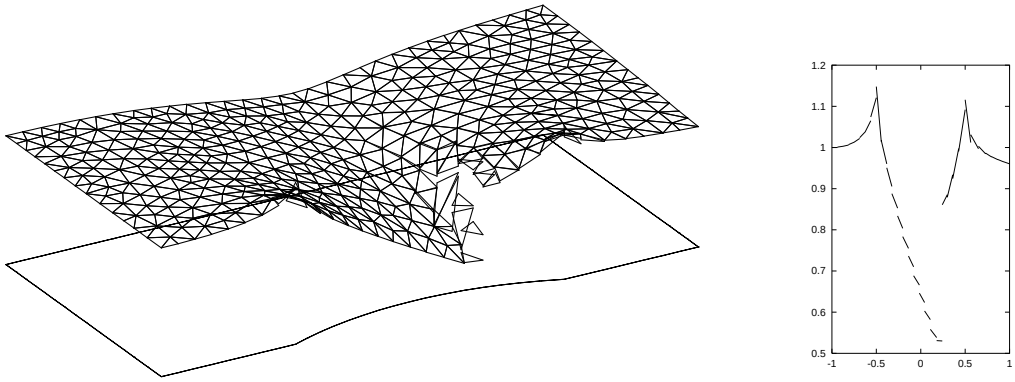

Figure 5: Distribution of the density in the computational domain (left) and along the lower wall (right) with the use of the superparametric FE for at $\partial\Omega$

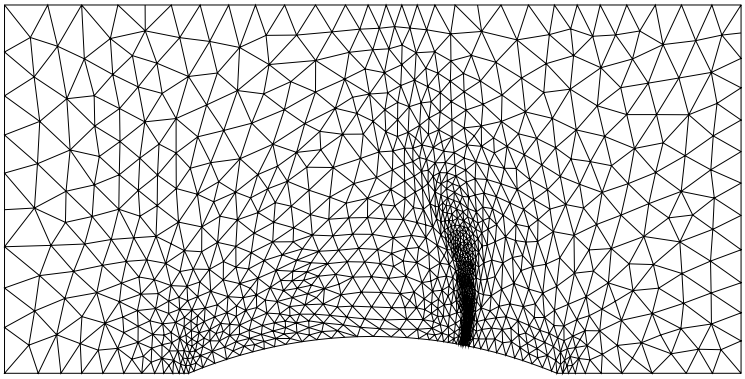

Figure 6: Adapted triangular mesh (2131 triangles)

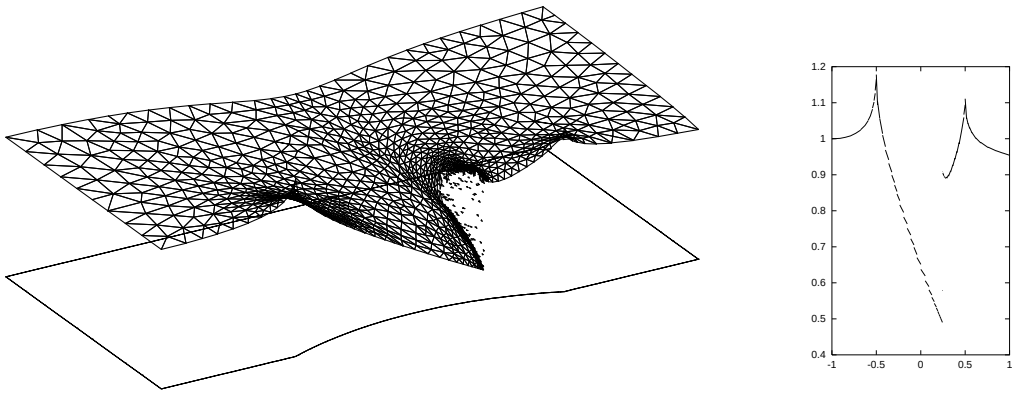

Figure 7: Distribution of the density in the computational domain (left) and along the lower wall (right) with superparametric FE on adapted mesh

$\#\mathcal{T}_h = 1766$), we obtain qualitatively good results. We observe very sharp capturing of shack wave (thanks adaptivity and discontinuous approximation) without any spurious oscillations. This example is a symmetric problem but the symmetry of the results is slightly smeared. It is caused by the fact, that the used triangulation is completely non symmetric (compare with Example 3, where symmetric mesh is employed).

Examples 3 In the last set of examples, the numerical scheme (4.6) was applied for the simulation of viscous flow around the profile NACA0012. The flow computation along NACA0012 profile was performed for the following sets of initial data, see [7]:

case	M_{in}	α	Re
C1	0.80	10°	500
C2	2.00	10°	106
C3	0.85	0°	500

where M_{in} is the inlet Mach number, α the angle of attack and Re the Reynolds number. We use the set of conditions (3.8) a)–b), (3.9) c'), where we consider free stream total temperature on the profile, i.e.,

$$\theta_D = \theta_\infty \left(1 + \frac{\gamma - 1}{2} M_\infty^2\right), \tag{6.2}$$

where θ_∞ and M_∞ are the value of temperature and Mach number at infinity, respectively. In order to avoid the influence of an artificial external boundary we choose the computational domain Ω with diameter twenty times larger then the diameter of the profile. We compare our results with the numerical results presented in [7], where ten authors presented their computations using different numerical method. The following table contains our computed lift c_L and drag c_R coefficients in comparison with [7] ($\#\mathcal{T}_h$ denotes the number of elements of $\#\mathcal{T}_h$)

		computed values		reference values from [7]	
case	$\#\mathcal{T}_h$	c_L	c_D	c_L	c_D
				range; mean value	(range); mean value
C1	4563	0.4985	0.1938	(0.4199 – 0.5170); 0.4526	(0.1597 – 0.2868); 0.2559
C2	5640	0.3969	0.4172	(0.3063 – 0.4059); 0.3443	(0.4120 – 0.4910); 0.4660
C3	4946	0.0003	0.2304	(0.0000 – 0.0007); 0.0001	(0.1790 – 0.2420); 0.2192

The computed values of c_L and c_D correspond with the reference ones. Figures 10 – 15 show the employed triangulations, computed isolines of the Mach number and density and the distributions of the density and the pressure coefficient along the profile. The isolines are not "smooth" which is caused by the fact that the used meshes are coarse and the visualization is performed without applying any smoothing mechanism. On the other hand, the distributions of ρ and c_p along profile are smooth as the meshes in vicinity of the profile are fine.

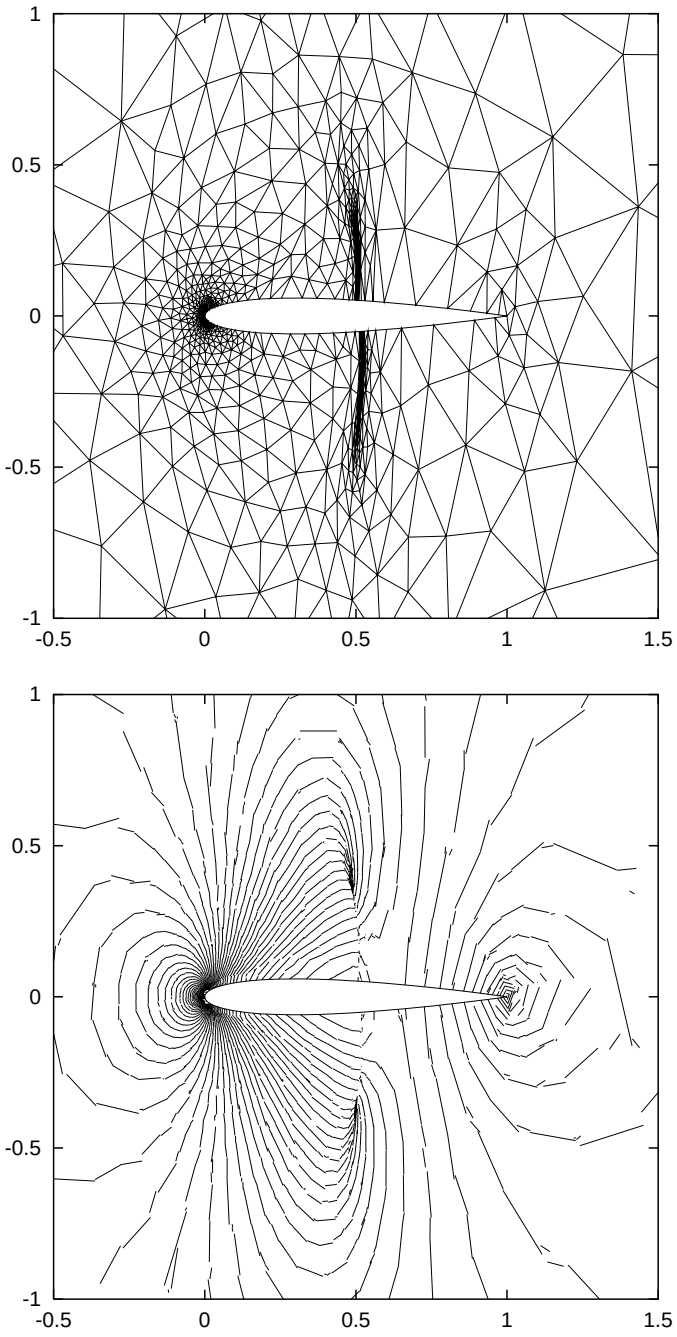

Figure 8: Inviscid flow along NACA 0012, $M_{\text{in}} = 0.8$, zero angle of attack, triangulation (top) and isolines of Mach number (bottom)

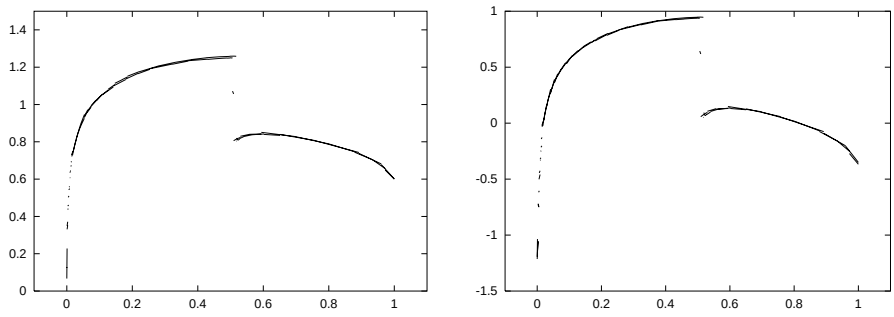

Figure 9: Inviscid flow along NACA 0012, $M_{\text{in}} = 0.8$, zero angle of attack, distribution of Mach number (left) and pressure coefficient (right) around the profile

7 Conclusion

We present the efficient numerical method for the solution of the compressible Euler and Navier-Stokes equations. The presented schemes are based on the discontinuous Galerkin finite element method.

We implemented piecewise linear approximation on unstructured triangular grids. An interesting observation is the following fact: although a discontinuous approximation is employed, the numerical solution looks continuous (i.e. interelement jumps are not visible) in subdomains where the solution is smooth. In order to avoid spurious oscillations in vicinity of discontinuities and steep gradients, the order limiting is applied. We can assume that the presented method is of the second order, see Remark 2.2. This property and the use of superparametric finite elements for curved parts of boundary produce satisfactory results even on coarse grids.

The drawback of the method is a high restriction on the time step given by the stability condition (3.30). Then in order to achieve the steady state solution, the high number of iterations has to be performed (in presented examples about $5 \cdot 10^4$). Therefore the future research should be devoted to the use of implicit schemes where the stability condition will be not so restrictive.

References

[1] Ph. Angot, V. Dolejší, M. Feistauer, and J. Felcman. Analysis of a combined barycentric finite volume – nonconforming finite element method for nonlinear convection-diffusion problems. *Appl. Math.*, 43(4):263–310, 1998.

[2] I. Babuška, C. E. Baumann, and J. T. Oden. A discontinuous *hp* finite element method for diffusion problems: 1-d analysis. *Computers and Mathematics with Applications*, 37:103–122, 1999.

[3] F. Bassi and S. Rebay. A high-order accurate discontinuous finite element method for the numerical solution of the compressible Navier–Stokes equations. *J. Comput. Phys*, 131:267–279, 1997.

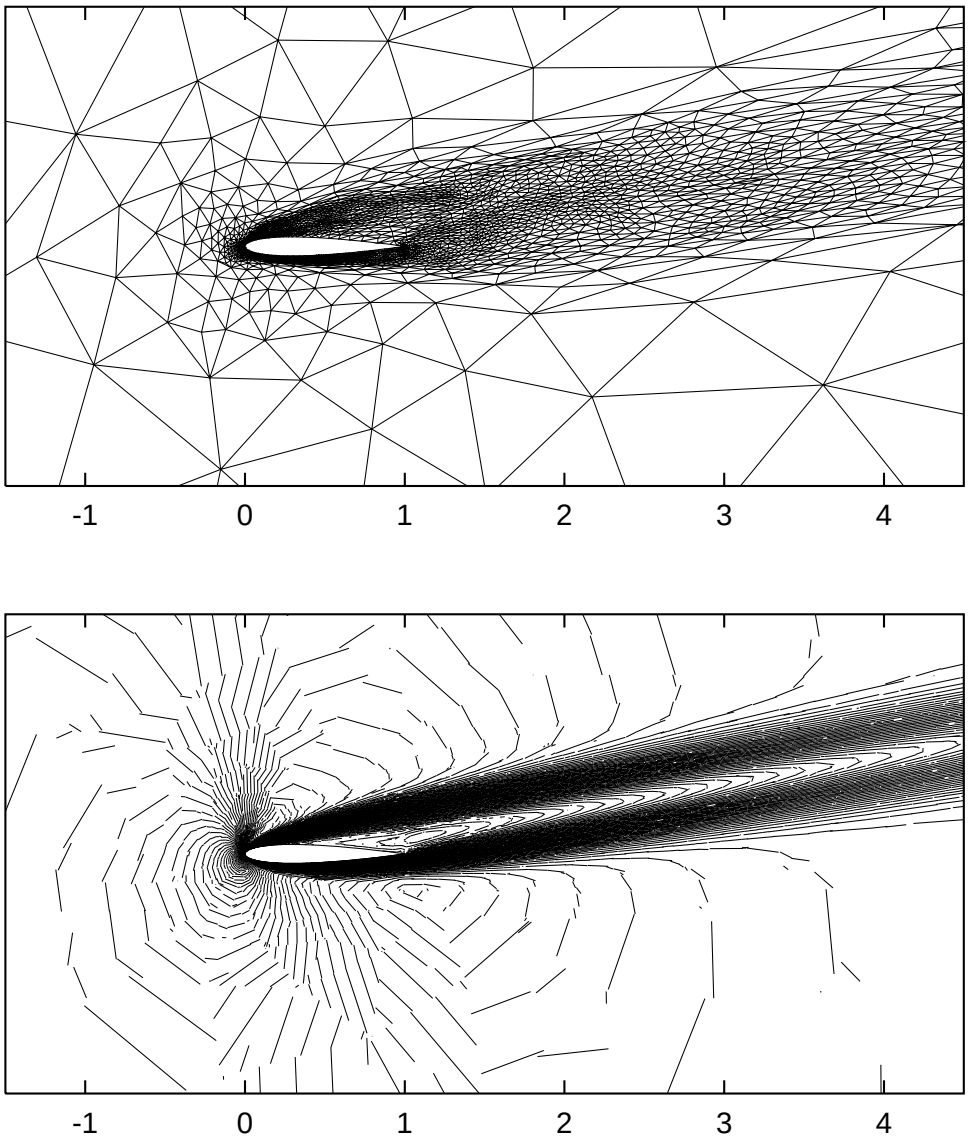

Figure 10: Viscous flow along NACA 0012, case C1, triangulation (top), isolines of Mach number (bottom)

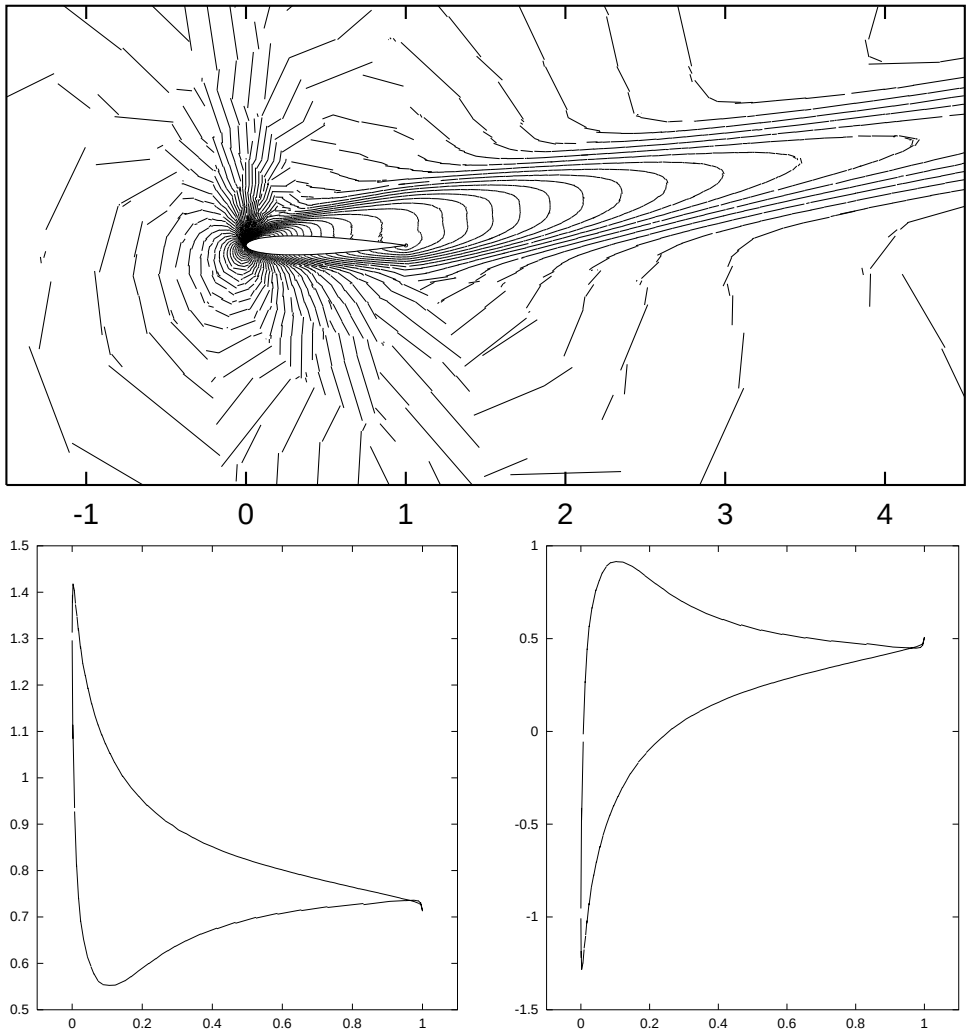

Figure 11: Viscous flow along NACA 0012, case C1, isolines of density (top), distribution of density (bottom left) and pressure coefficient (bottom right) along the profile

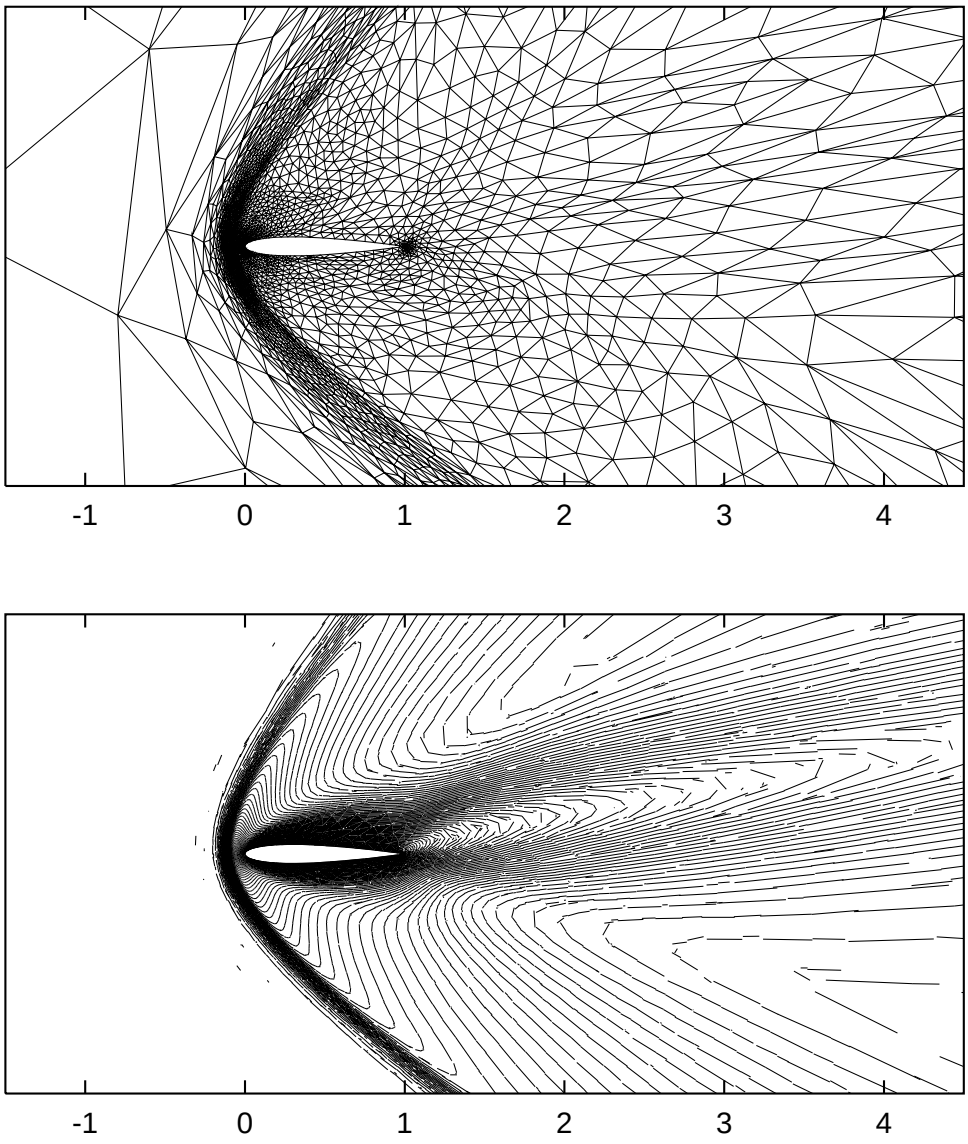

Figure 12: Viscous flow along NACA 0012, case C2, triangulation (top), isolines of Mach number (bottom)

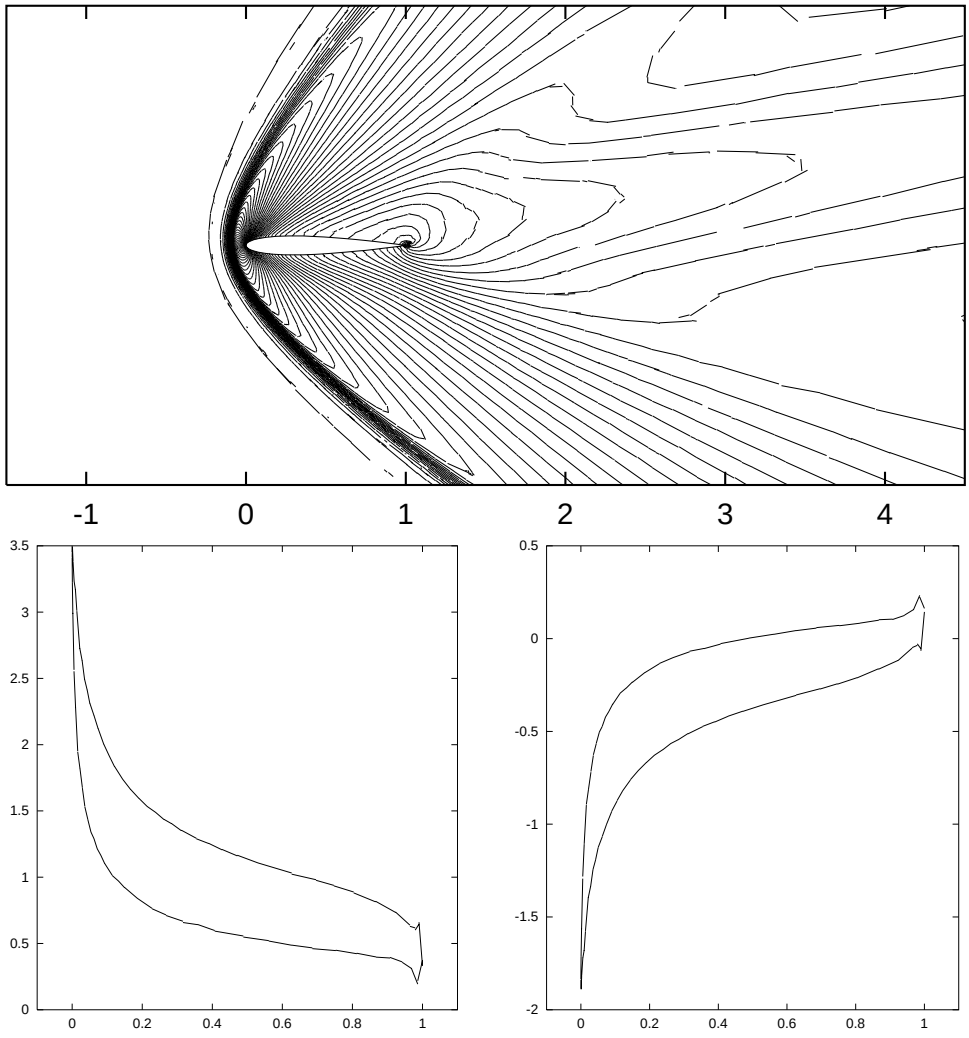

Figure 13: Viscous flow along NACA 0012, case C2, isolines of density (top), distribution of density (bottom left) and pressure coefficient (bottom right) along the profile

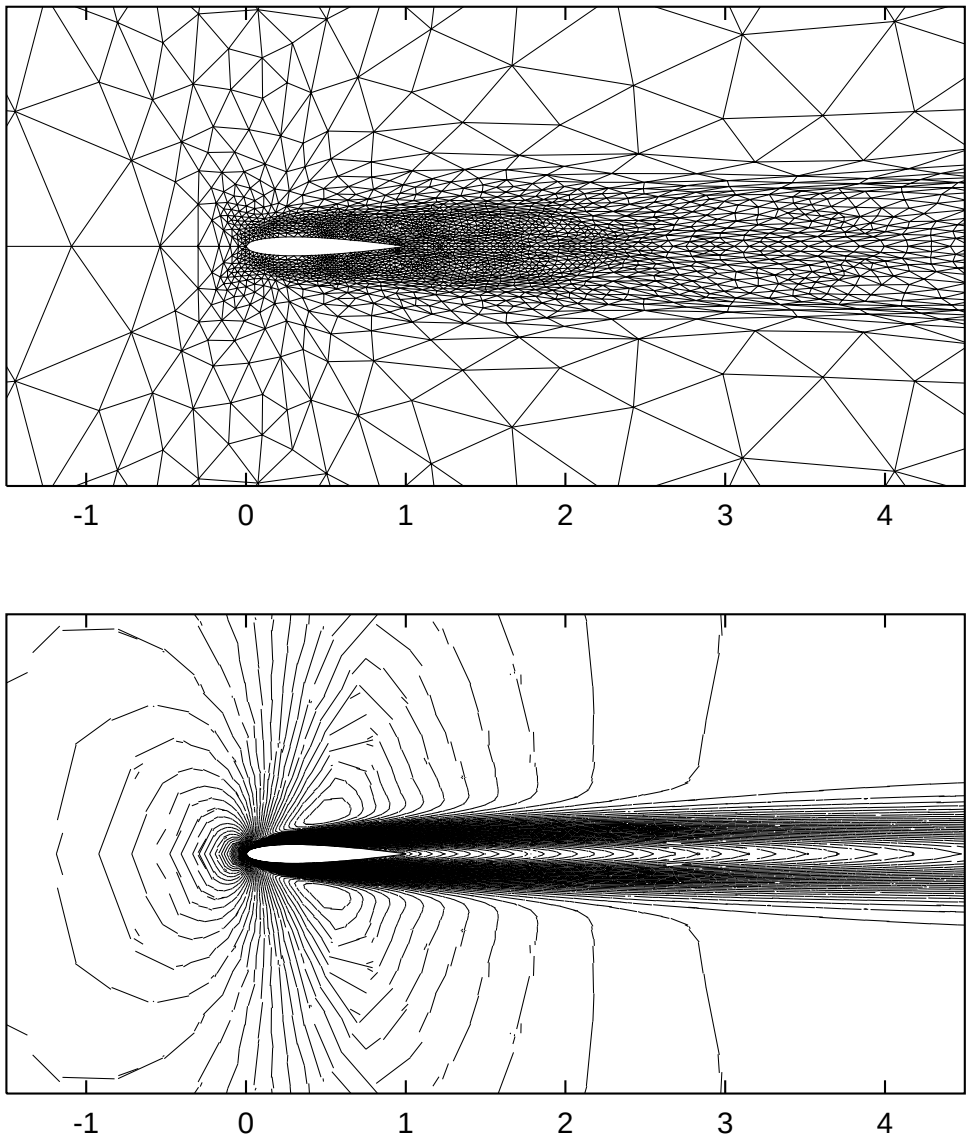

Figure 14: Viscous flow along NACA 0012, case C3, triangulation (top), isolines of Mach number (bottom)

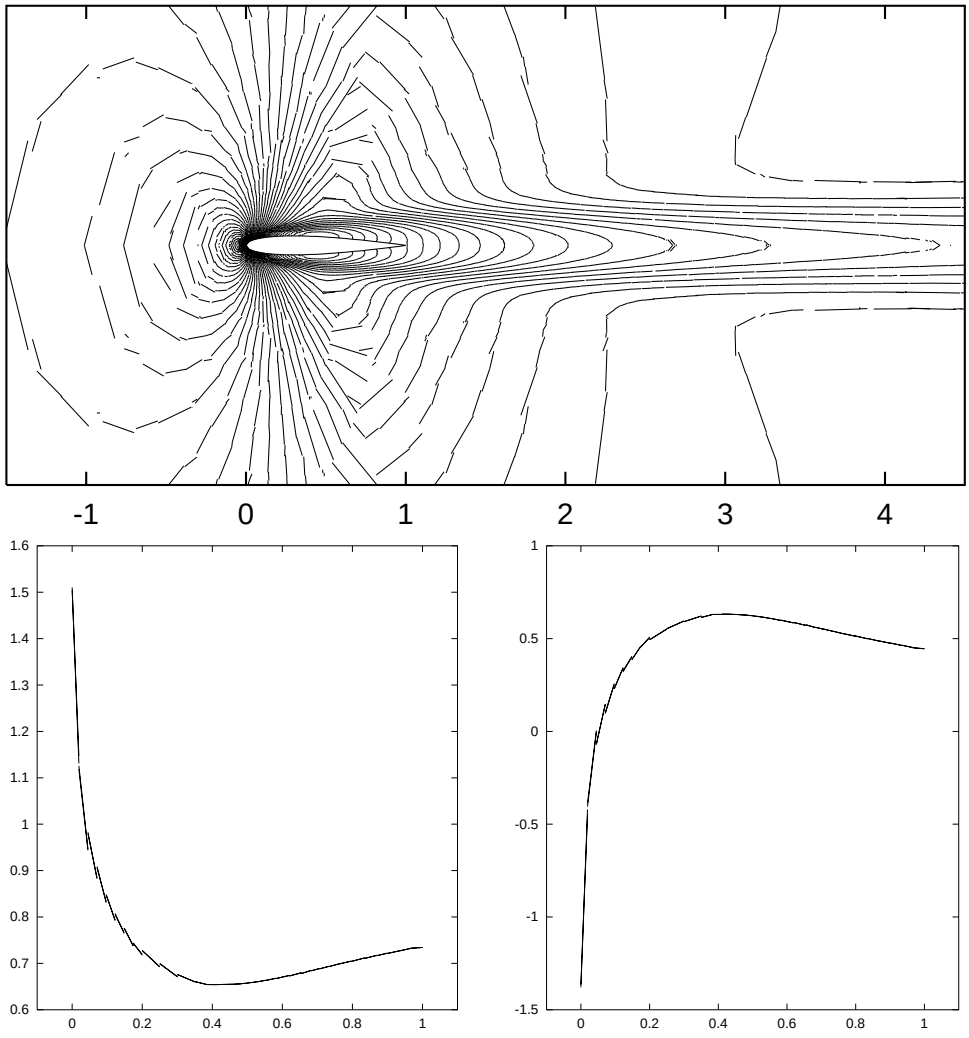

Figure 15: Viscous flow along NACA 0012, case C3, isolines of density (top), distribution of density (bottom left) and pressure coefficient (bottom right) along the profile

[4] F. Bassi and S. Rebay. A high order discontinuous Galerkin method for compressible turbulent flow. In M. Griebel, D. E. Keyes, R. M. Nieminen, D. Rose, and T. Schlick, editors, *Discontinuous Galerkin Method: Theory, Computations and Applications, Lecture Notes in Computation Science and Engineering*. Springer-Verlag, 2000.

[5] C. E. Baumann and J. T. Tinsley. A discontinuous *hp* finite element method for the Euler and Navier-Stokes equations. *Int. J. Numer. Methods Fluids*, 31(1):79–95, 1999.

[6] F. Brezzi, G. Manzini, D. Marini, P. Pietra, and A. Russo. Discontinuous Galerkin approximations for elliptic problems. *Numer. Methods Partial Differ. Equations*, 16:35–378, 2000.

[7] M. O. Bristeau, R. Glowinski, J. Periaux, and H. Viviand, editors. *Numerical Simulation of Compressible Navier-Stokes Flows*, volume 18 of *Notes on Numerical Fluid Mechanics*. Vieweg, Braunschwig, 1987.

[8] B. Cockburn. Discontinuous Galerkin methods for convection dominated problems. In T. J. Barth and H. Deconinck, editors, *High–Order Methods for Computational Physics*, number 9 in Lecture Notes in Computational Science and Engineering, pages 69–224. Springer, Berlin, 1999.

[9] B. Cockburn, G. E. Karniadakis, and C.-W. Shu (eds.). Discontinuous Galerkin methods. In *Lecture Notes in Computational Science and Engineering 11*. Springer, Berlin, 2000.

[10] V. Dolejší. Anisotropic mesh adaptation for finite volume and finite element methods on triangular meshes. *Computing and Visualization in Science*, 1(3):165–178, 1998.

[11] V. Dolejší. Anisotropic mesh adaptation technique for viscous flow simulation. *East-West Journal of Numerical Mathematics*, 9(1):1–24, 2001.

[12] V. Dolejší, M. Feistauer, and C. Schwab. A discontinuous Galerkin method for nonlinear convection–diffusion problems. (in preparation).

[13] V. Dolejší, M. Feistauer, and C. Schwab. A finite volume discontinuous Galerkin scheme for nonlinear convection–diffusion problems. *Calcolo*, 39:1–40, 2002.

[14] V. Dolejší and J. Felcman. Numerical methods for hyperbolic systems - application in fluid dynamics. *Engineering MECHANICS*, 9(3):139–152, 2002.

[15] V. Dolejší, M. Feistauer, and C. Schwab. On some aspects of the discontinuous Galerkin finite element method for conservation laws. *The Preprint Series of the School of Mathematics, Charles University Prague, No. MATH–KNM–2001/5*, 2001. (to appear in Mathematics and Computers in Simulation).

[16] M. Feistauer. *Mathematical Methods in Fluid Dynamics*. Longman Scientific & Technical, Harlow, 1993.

[17] M. Feistauer. Numerical methods for compressible flow. In J. Neustupa and P. Penel, editors, *Mathematical Fluid Mechanics. Recent Results and Open Questions*. Birkhäuser, Basel, 2001.

[18] M. Feistauer and J. Felcman. Convection-Diffusion Problems and Compressible Navier–Stokes Equations. In J. R. Whitemen, editor, *The Mathematics of Finite Elements and Applications*, pages 175–194. John Wiley & Sons, 1996.

[19] M. Feistauer, J. Felcman, and V. Dolejší. Numerical simulation of compresssible viscous flow through cascades of profiles. *ZAMM*, 76(S4):297–300, 1996.

[20] M. Feistauer, J. Felcman, and M. Lukáčová-Medvidová. On the convergence of a combined finite volume – finite element method for nonlinear convection – diffusion problems. *Numer. Methods Partial Differ. Equations*, 13:163–190, 1997.

[21] M. Feistauer, J. Felcman, M. Lukáčová-Medvidová, and G. Warnecke. Error estimates of a combined finite volume – finite element method for nonlinear convection – diffusion problems. *SIAM J. Numer. Anal.*, 36(5):1528–1548, 1999.

[22] M. Feistauer, J. Felcman, and M. Lukáčová. Combined finite element–finite volume solution of compressible flow. *J. Comput. Appl. Math.*, 63:179–199, 1995.

[23] J. Felcman. Grid refinement–alignment in 3D flow computations. *Mathematics and Computers in Simulation*, (to appear).

[24] R. Hartmann and P. Houston. Adaptive discontinuous Galerkin finite element methods for nonlinear hyperbolic conservation laws. *Preprint 2001–20 (SFB 359), IWR Heidelberg*, 2001. (submitted to SIAM J. Sci. Comp.).

[25] P. Houston, C. Schwab, and E. Süli. Discontinuous $hp--$finite element method for advection–diffusion problems. Technical Report Research Report No. 2000–07, SAM ETH Zürich, 2000.

[26] J. T. Oden, I. Babuška, and C. E. Baumann. A discontinuous *hp* finite element method for diffusion problems. *J. Comput. Phys*, 146:491–519, 1998.

[27] E. F. Toro. *Riemann Solvers and Numerical Methods for Fluid Dynamics*. Springer-Verlag, 1997.

List of preprints released in this series

All preprints available on http://www.karlin.mff.cuni.cz/ms-preprints/
E-mail contact to series administrator: knm-prep@karlin.mff.cuni.cz

[MATH-kma-2002/1] W.Desch, E. Fasanga, J.Milota: *Unbounded observers and Riccati operators in nonreflexive spaces* (07.01.2002)

[MATH-kma-2002/2] Amiran Gogatishvili, Lubos Pick: *Discretization and anti-discretization of rearrangement-invariant norms* (07.01.2002)

[MATH-MU-2002/1] J. Hron, J. Málek, J. Nečas, K.R. Rajagopal: *Numerical Simulations and Global Existence of Solutions of Two Dimensional Flows of Fluids with Pressure and Shear Dependent Viscosities* (27.02.2002)

[MATH-alg-2002/1] A.Drapal: *On multiplication groups of relatively free quasigroups isotopic to abelian groups* (08.03.2002)

[MATH-alg-2002/2] J. Tuma and F. Wehrung: *A survey of recent results on congruence lattices of lattices* (13.03.2002)

[MATH-alg-2002/3] M. Semenova and F.Wehrung: *Sublattices of lattices of order-convex sets, I. The main representation theorem* (13.03.2002)

[MATH-alg-2002/4] M. Semenova and F.Wehrung: *Sublattices of lattices of order-convex sets, II. Posets of finite length* (13.03.2002)

[MATH-knm-2002/1] Vit Dolejsi and Miloslav Feistauer: *On the Discontinuous Galerkin Method for the Numerical Solution of Compressible High-Speed Flow* (20.03.2002)

[MATH-kma-2002/76] Marian Fabian, Ondrej Kalenda, Jiri Kolar: *Filling analytic sets by the derivatives of C^1-smooth bumps* (27.03.2002)

[MATH-alg-2002/5] S.Holub: *Binary equality set is generated by two words* (11.04.2002)

[MATH-kma-2002/77] Ales Nekvinda, Ludek Zajicek: *Gateaux differentiability of Lipschitz functions via directional derivatives* (17.04.2002)

[MATH-alg-2002/6] A.Drapal: *The entwining snake is reborn* (19.04.2002)

[MATH-kma-2002/78] Jaroslav Lukes, Ivan Netuka, Jiri Vesely: *Choquet's theory and the Dirichlet problem* (24.04.2002)

[MATH-MU-2002/2] Petr Somberg: *The generalized $_\infty$-algebra structure on BGG sequences and graph sequence of generalized associative operad* (06.05.2002)

[MATH-kma-2002/79] Stanislav Hencl: *A sharp form of an embedding into exponential and double exponential spaces* (16.05.2002)

[MATH-kma-2002/80] Jiri Spurny: *Representation of abstract affine functions* (16.05.2002)

[MATH-kma-2002/81] M. E. Mera, M. Moran, D. Preiss, L. Zajicek: *Porosity, σ-porosity and measures* (28.05.2002)

[MATH-MU-2002/3] J. Rataj, M. Zähle: *Normal cycles of Lipschitz manifolds by approximation with parallel sets* (13.06.2002)

[MATH-MU-2002/4] J. Bureš, J. Vanžura: *Multisymplectic forms of degree three in dimension seven* (19.06.2002)

[MATH-alg-2002/7] Lidia Angeleri Huegel and Jan Trlifaj: *Direct limits of modules of finite projective dimension* (10.07.2002)

[MATH-alg-2002/8] M. Semenova and F.Wehrung: *Sublattices of lattices of order-convex sets, III. The case of totaly ordered sets* (11.07.2002)

[MATH-alg-2002/9] Jan Trlifaj: *Ext and inverse limits* (02.09.2002)

[MATH-kma-2002/82] Jan Rychtar: *On the invariant subspaces of $B(X)$ in X^{**}* (13.09.2002)

[MATH-kma-2002/83] Petr Hajek, Jan Rychtar: *On a problem of Borwein* (25.09.2002)

[MATH-alg-2002/10] Jan Zemlicka: *Which regular semiartinian rings with primitive factors artinian exist?* (30.09.2002)

[MATH-kma-2002/84] Petr Holicky, Jan Pelant: *Internal descriptions of absolute Borel classes* (02.10.2002)

[MATH-kma-2002/85] Stanislav Hencl: *Explicit upper bound for entropy numbers* (05.10.2002)

[MATH-kma-2002/87] Ales Nekvinda, Ludek Zajicek: *Extensions of real and vector functions of one variable which preserve differentiability* (05.11.2002)

[MATH-kma-2002/86] Jan Kolar, Jan Kristensen: *Gradient ranges of bumps on the plane* (05.11.2002)

[MATH-kma-2002/88] Stanislav Hencl: *Notes on absolutely continuous functions of several variables* (06.11.2002)

[MATH-MU-2002/5] P.Somberg: *Contact symplectic parabolic geometry* (07.11.2002)

[MATH-MU-2002/6] M.Pokorny: *On the result of He concerning the smoothness of solutions to the Navier-Stokes equations* (07.11.2002)